

Nicotinamide phosphoribosyltransferase inhibitors, design, preparation and SAR.

Christensen, Mette Knak; Erichsen, Kamille Dumong; Olesen, Uffe Høgh; Tjørnelund, Jette; Fristrup, Peter; Thougard, Annemette; Nielsen, Søren Jensby; Sehested, Maxwell; Jensen, Peter B.; Loza, Einars; Kalvinsh, Ivars; Garten, Antje; Kiess, Wieland; Bjorkling, Fredrik

Published in:
Open Journal of Medicinal Chemistry

Link to article, DOI:
[10.1021/jm4009949](https://doi.org/10.1021/jm4009949)

Publication date:
2013

Document Version
Publisher's PDF, also known as Version of record

[Link back to DTU Orbit](#)

Citation (APA):
Christensen, M. K., Erichsen, K. D., Olesen, U. H., Tjørnelund, J., Fristrup, P., Thougard, A., ... Bjorkling, F. (2013). Nicotinamide phosphoribosyltransferase inhibitors, design, preparation and SAR. Open Journal of Medicinal Chemistry, 56(22), 9071–9088. DOI: 10.1021/jm4009949

DTU Library

Technical Information Center of Denmark

General rights

Copyright and moral rights for the publications made accessible in the public portal are retained by the authors and/or other copyright owners and it is a condition of accessing publications that users recognise and abide by the legal requirements associated with these rights.

- Users may download and print one copy of any publication from the public portal for the purpose of private study or research.
- You may not further distribute the material or use it for any profit-making activity or commercial gain
- You may freely distribute the URL identifying the publication in the public portal

If you believe that this document breaches copyright please contact us providing details, and we will remove access to the work immediately and investigate your claim.

Nicotinamide phosphoribosyltransferase inhibitors, design, preparation and SAR.

Mette Knak Christensen, Kamille Dumong Erichsen, Uffe Høgh Olesen, Jette Tjørnelund, Peter Fristrup, Annemette Thougard, Søren Jensby Nielsen, Maxwell Sehested, Peter Buhl Jensen, Einars Loza, Ivars Kalvinsh, Antje Garten, Wieland Kiess, and Fredrik Bjorkling

J. Med. Chem., **Just Accepted Manuscript** • Publication Date (Web): 28 Oct 2013

Downloaded from <http://pubs.acs.org> on November 12, 2013

Just Accepted

“Just Accepted” manuscripts have been peer-reviewed and accepted for publication. They are posted online prior to technical editing, formatting for publication and author proofing. The American Chemical Society provides “Just Accepted” as a free service to the research community to expedite the dissemination of scientific material as soon as possible after acceptance. “Just Accepted” manuscripts appear in full in PDF format accompanied by an HTML abstract. “Just Accepted” manuscripts have been fully peer reviewed, but should not be considered the official version of record. They are accessible to all readers and citable by the Digital Object Identifier (DOI®). “Just Accepted” is an optional service offered to authors. Therefore, the “Just Accepted” Web site may not include all articles that will be published in the journal. After a manuscript is technically edited and formatted, it will be removed from the “Just Accepted” Web site and published as an ASAP article. Note that technical editing may introduce minor changes to the manuscript text and/or graphics which could affect content, and all legal disclaimers and ethical guidelines that apply to the journal pertain. ACS cannot be held responsible for errors or consequences arising from the use of information contained in these “Just Accepted” manuscripts.



Nicotinamide phosphoribosyltransferase inhibitors, design, preparation and SAR.

Mette K. Christensen,[†] Kamille D. Erichsen,[†] Uffe H. Olesen,^{†,§} Jette Tjørnelund,[†] Peter

Frstrup,[□] Annemette Thougard,[†] Søren Jensby Nielsen,[†] Maxwell Sehested,^{†,§} Peter B. Jensen,[†]

Einars Loza,^ψ Ivars Kalvinsh,^ψ Antje Garten,^λ Wieland Kiess,^λ and Fredrik Björkling.^{†,‡,*}

[†]Topotarget A/S, Symbion, Fruebjergvej 3, DK-2100 Copenhagen, Denmark

[‡]Department of Drug Design and Pharmacology, Faculty of Health and Medical Sciences, University of Copenhagen, Universitetsparken 2, DK-2100 Copenhagen, Denmark

[§]Experimental Pathology Unit, National University Hospital, Biocentre, Ole Maaloes Vej 5, DK-2200 Copenhagen, Denmark

^λ Center for Pediatric Research, Hospital for Children and Adolescents, University of Leipzig, Liebigstr. 21, 04301 Leipzig, Germany

[□]Department of Chemistry, Technical University of Denmark, Kemitorvet 207, DK-2800 Lyngby, Denmark

^ψLatvian Institute of Organic Synthesis, Aizkraukles 21, LV-1006 Riga, Latvia

KEYWORDS: Cancer, medicinal chemistry, nicotinamide phosphoribosyltransferase, NAMPT, nicotinamide adenine dinucleotide (NAD), mouse xenograft.

Abstract.

Existing pharmacological inhibitors for nicotinamide phosphoribosyltransferase (NAMPT) are promising therapeutics for treating cancer. Using medicinal and computational chemistry methods, the structure-activity relationship for novel classes of NAMPT inhibitors is described and compounds optimized. Compounds are designed inspired by the NAMPT inhibitor APO866 and cyanoguanidine inhibitor scaffolds. In comparison with recently published derivatives the new analogues exhibit an equally potent anti-proliferative activity in vitro and comparable activity in vivo. The best performing compounds from these series showed sub-nanomolar anti-proliferative activity towards a series of cancer cell-lines (compound **15**: IC₅₀ 0.025 nM and 0.33 nM, in A2780 (ovarian carcinoma) and MCF-7 (breast), respectively), and potent anti-tumour in vivo activity in well tolerated doses in a xenograft model. In an A2780 xenograft mouse model with large tumours (500 mm³) compound **15** reduced the tumour volume to one fifth of the starting volume at a dose of 3 mg/kg administered i.p., bid, day 1-9. Thus, compounds found in this study compared favourably with compounds already in the clinic and warrant further investigation as promising lead molecules for the inhibition of NAMPT.

Introduction

Inhibition of nicotinamide adenine dinucleotide, (NAD) production has recently been suggested as a principle for inducing death of cells with high demand for this dinucleotide.¹ This is particularly true for cancer cells due to increased metabolism and high activity of NAD consuming enzymes. NAD is an essential cofactor in redox reactions and as such involved in cellular energy production and metabolism without being substantially consumed. However, besides being a cofactor, NAD serves as the substrate for mono-ADP-ribosyltransferases,² poly-ADP-ribose polymerases (PARPs),³ and sirtuins,⁴ all of these converting NAD to nicotinamide. Also, NAD is consumed as the precursor for a number of Ca²⁺-releasing second messengers (e.g., cADPR, NAADP).^{5,6}

1 Thus, the increased dependence on glycolysis and elevated expression or activity of PARPs,⁷⁻⁹ and
2 sirtuins,⁴ characteristic for malignant cells, make these more sensitive to NAD availability as compared
3 with normal cells.^{10,11}

4
5
6
7 In the organism several pathways for the synthesis of NAD are known. Besides the "de novo" pathway
8 using tryptophan as precursor, NAD can alternatively be synthesized or resynthesized from
9 nicotinamide, a sequence where Nicotinamide phosphoribosyltransferase (NAMPT) catalyzes the rate
10 limiting step.¹²⁻¹⁴ Thus, inhibition of NAMPT enzyme activity causes a direct inhibition of NAD
11 production. Importantly, normal cells can use an alternative pathway for NAD synthesis from nicotinic
12 acid (NA), catalyzed by nicotinic acid phosphoribosyltransferase (NAPRT).¹⁵⁻¹⁷ Unlike most normal
13 tissues many cancer cell lines, and primary tumours, are deficient in NAPRT activity.¹⁸ Furthermore, an
14 increased concentration of NAMPT in colorectal, ovarian, and prostate cancer cells has been
15 reported.^{10,19, 20} Altogether, inhibition of NAD production via NAMPT inhibition is suggested to be a
16 valid principle for selective inhibition of cancer cell growth and as such represents an attractive target
17 for drug discovery.
18
19
20
21
22
23
24
25
26
27
28
29
30
31
32
33
34

35 A few classes of NAMPT inhibitors have been reported such as compounds APO866 (**1**)²¹ and CHS828,
36 (**2**)²² which have entered the clinic, and more recent structures like TRON-8²³ and CB30865²⁴ for which
37 biological data have been reported (Figure 1). Biological data for NAMPT inhibitor MCP-8640 is also
38 reported but no chemical structure.²⁵ These NAMPT inhibitors show potent anti-proliferative activity in
39 a spectrum of cancer cell lines and in vivo efficacy in both solid tumours and leukemia in preclinical
40 studies.^{26,27} A comprehensive literature review on NAMPT inhibitors including patents was recently
41 published.²⁸ Originally, **1** was developed as an inhibitor of NAMPT and displays anti-proliferative
42 activities comparable to compound **2** for which the molecular target was unknown until recently.²⁹⁻³¹
43 Safety, pharmacokinetics and biological effect of compound **1** and **2** (and a pro-drug thereof, **3**, Figure
44 1) have been reported from five phase I clinical trials performed in patients with advanced disease.³²⁻³⁴
45 In these trials, not surprisingly in phase I, no objective response was found and for both compounds the
46
47
48
49
50
51
52
53
54
55
56
57
58
59
60

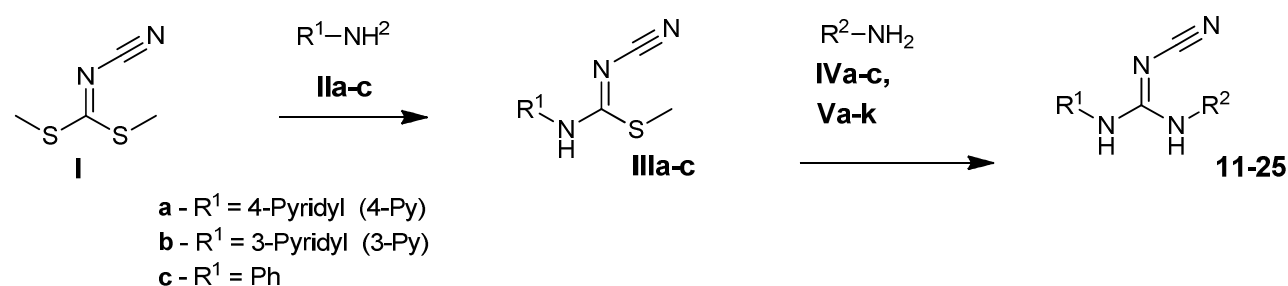
Results and discussion

Chemistry

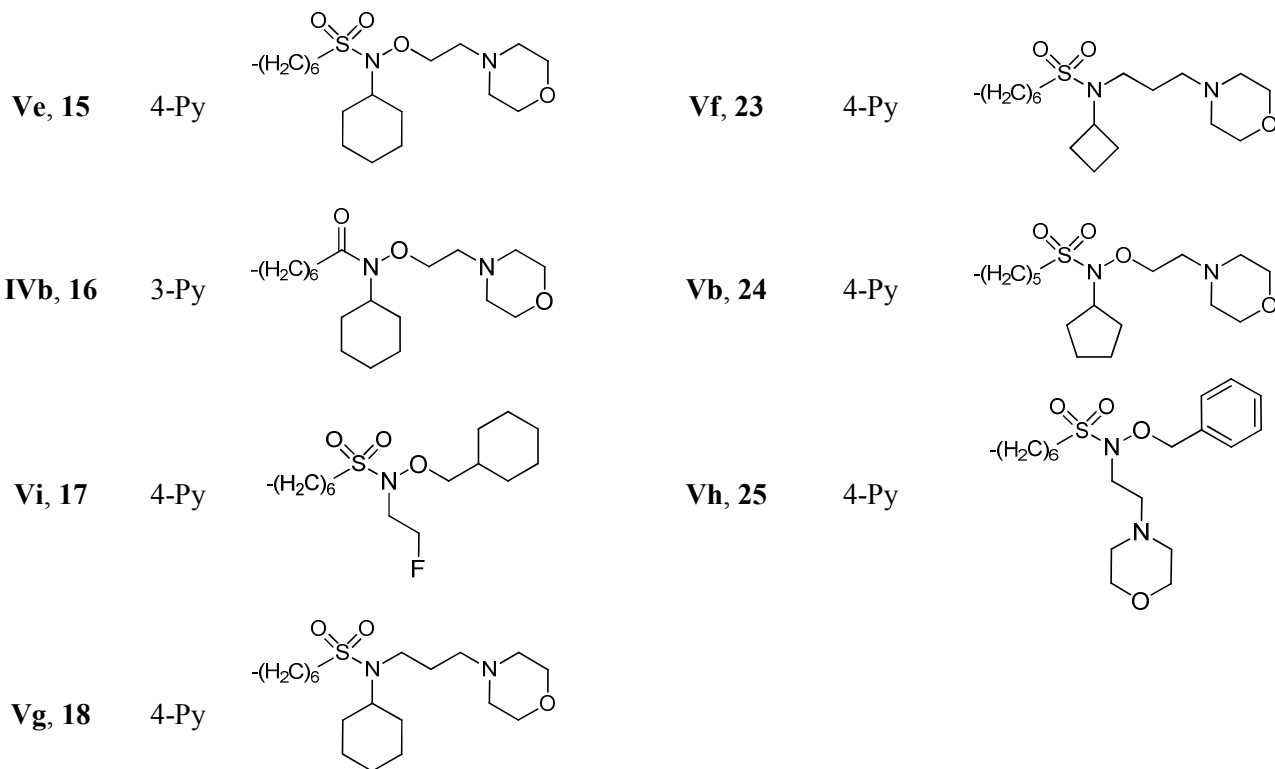
A series of 2-cyanoguanidines **11-25** was synthesized using a general strategy (Scheme 1, Table 1).

Treatment of dimethyl cyanocarbonimidodithioate (**I**) with 4-pyridylamine (**IIa**), 3-pyridylamine (**IIb**) or aniline (**IIc**) produced methyl *N'*-cyano-*N*-arylcarbamiimidodithioates **IIIa-c**, which were condensed with pre-assembled hydroxamate amines **IVa-c** or sulfonamide amines **Va-k** to give the corresponding 2-cyanoguanidines **11-25**.

Scheme 1. Convergent Synthesis of 2-Cyanoguanidine Derivatives 11-25



No	R ¹	R ²	No	R ¹	R ²
IVc, 11	4-Py		Vj, 19	4-Py	
IVa, 12	4-Py		Va, 20	4-Py	
IVb, 13	Ph		Vd, 21	4-Py	
Vk, 14	4-Py		Vc, 22	4-Py	

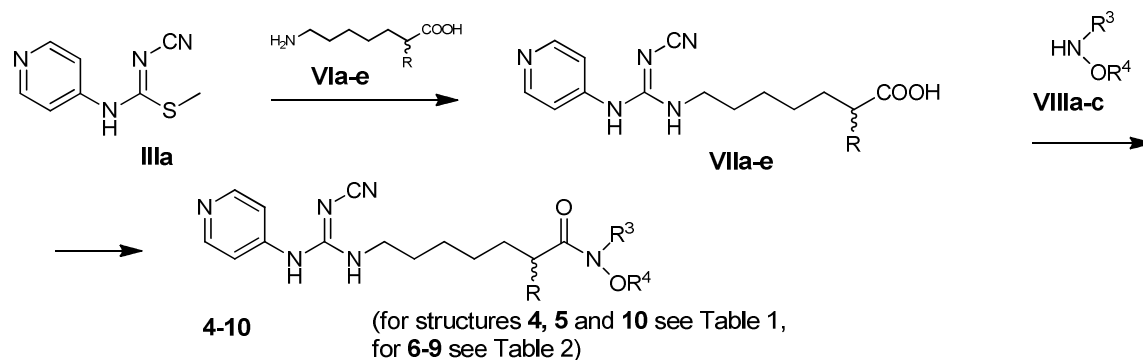


Although this convergent approach was successful in most cases, a stepwise formation of the side chain was used for some 2-cyanoguanidine derivatives such as **4-10** (Scheme 2, Tables 1 and 2).

Thus, the condensation of methyl *N*-cyano-*N*-(pyridin-4-yl)carbamiimidothioate (**IIIa**) with 7-aminoheptanoic acid (**VIa**) or optically active 2-methyl or 2-benzyl-7-aminoheptanoic acids **VIb-e**³⁸ produced 7-guanidinoheptanoic acid derivatives **VIIa-e**. These intermediate acids **VIIa-e** afforded the target *N*-hydroxycarboxamides **4-10** when treated with hydroxylamines **VIIIa-c** in the presence of 1-ethyl-3-(3-dimethylaminopropyl)carbodiimide (EDC) or *O*-(7-azabenzotriazol-1-yl)-*N,N,N',N'*-tetramethyluronium hexafluorophosphate (HATU).

Scheme 2. Synthesis of 2-Cyanoguanidine Derivatives 4-10 via Carboxylic Acid Intermediates

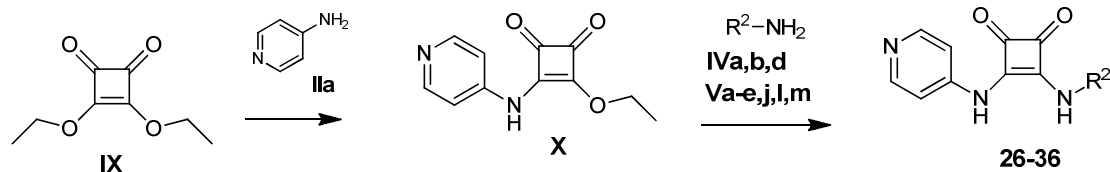
VIIa-e



No	R	No	R ³	R ⁴	No	R	R ³	R ⁴
VIa, VIIa	H	VIIIa	H		4	H	H	
VIb, VIIb	(R)-Me	VIIIb	Bn		5	H	Bn	
VIc, VIIc	(S)-Me	VIIIc			6	(S)-Me	H	
VIe, VIIe	(S)-Bn				7	(R)-Me	H	
					8	(S)-Bn	H	
					9	(R)-Bn	H	
					10	H		

A similar convergent approach to Scheme 1 was used for the preparation of a series of 1,2-diaminocyclobutene-3,4-diones **26-36** (Scheme 3, Table 3).³⁹ Reaction of 3,4-diethoxy-3-cyclobutene-1,2-dione (**IX**) with 4-pyridylamine (**IIa**) afforded intermediate amidoester **X**, which was treated with amines **IVa,b,d**, **Va-e,j,l,m** to obtain target 1,2-diaminocyclobutene-3,4-diones **26-36**.

Scheme 3. Convergent Synthesis of 1,2-Diaminocyclobutene-3,4-dione derivatives 26-36

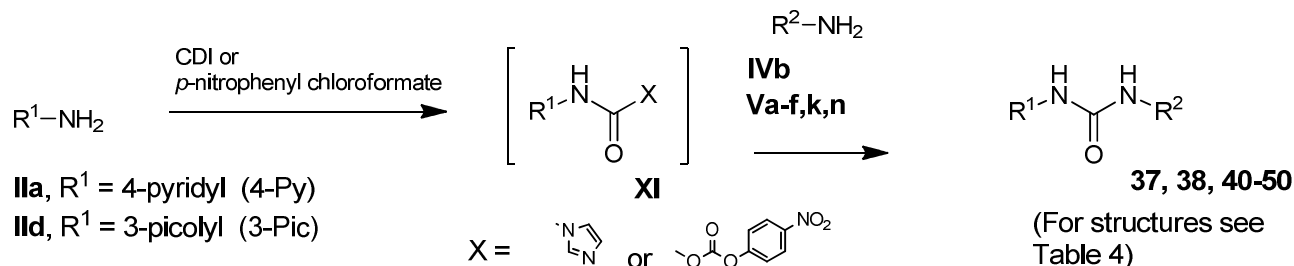


(for structures see
Table 3)

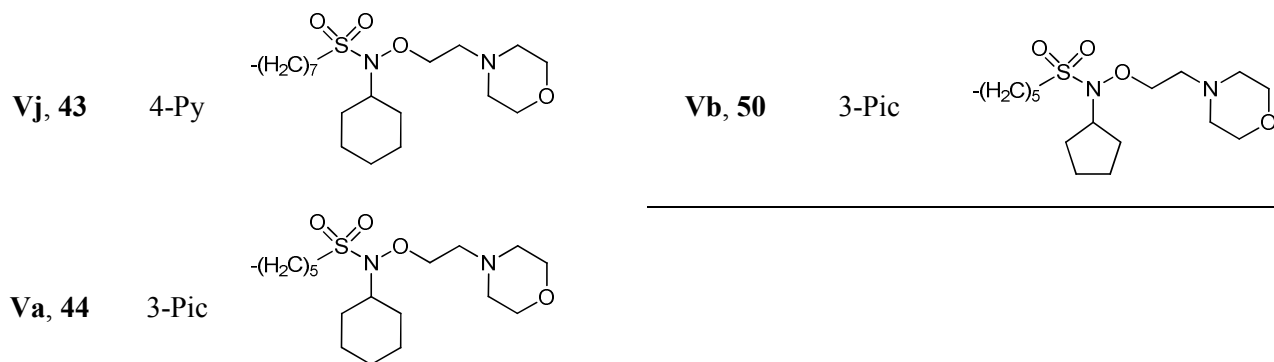
No	R ²	No	R ²
IVb, 26		Vj, 32	
VI, 27		Va, 33	
IVd, 28		Vd, 34	
IVa, 29		Vc, 35	
Vm, 30		Vb, 36	
Ve, 31			

N,N'-Disubstituted urea derivatives **37**, **38**, **40-50** (Table 4) were prepared by reacting of such carbonic acid derivatives as *N,N'*-carbonyldiimidazole (CDI) or 4-nitrophenyl chloroformate with 4-pyridylamine (**IIa**) or 3-picolylamine (**IIc**) followed by appropriate pre-assembled amines **IVb**, **Va-f,k,n** (Scheme 4).

Scheme 4. Synthesis of *N,N'*-Disubstituted Urea Derivatives **37**, **38**, **40-50**



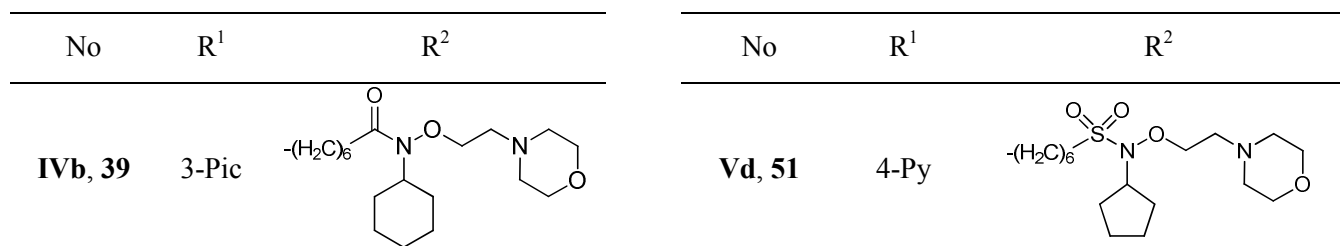
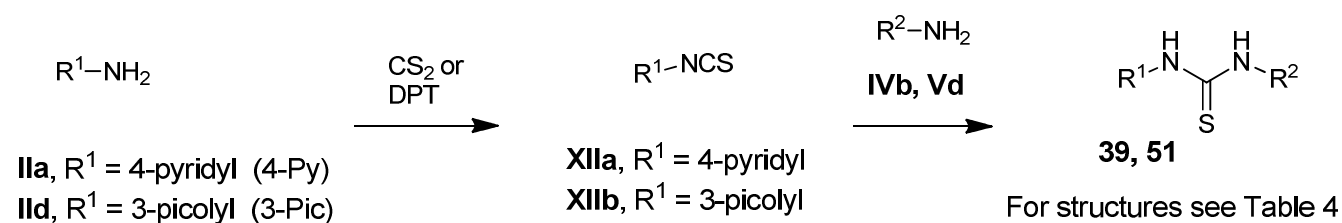
No	R ¹	R ²	No	R ¹	R ²
Ve, 37	4-Py		Vj, 45	3-Pic	
IVb, 38	3-Pic		Vd, 46	3-Pic	
Vm, 40	4-Py		Vc, 47	3-Pic	
Vm, 41	3-Pic		Vf, 48	3-Pic	
Va, 42	4-Py		Vn, 49	3-Pic	



15
16
17
18
19
20
21
22
23
24
25
26
27
28
29
30
31
32

The *N,N'*-disubstituted thiourea derivative **39** was synthesized by the condensation of 3-picolylamine **IId** with di(2-pyridyl) thionocarbonate (DPT) followed by treatment of *in situ* formed intermediate isothiocyanate **XIIb** with amine **IVb**. The *N,N'*-disubstituted thiourea derivative **51** was prepared from amine **Vd** and isothiocyanate **XIIa**, which in turn was obtained from 4-pyridilamine **IIa** and carbon disulfide (Scheme 5, Table 4).

Scheme 5. Synthesis of *N,N'*-Disubstituted Thiourea Derivatives **39** and **51**

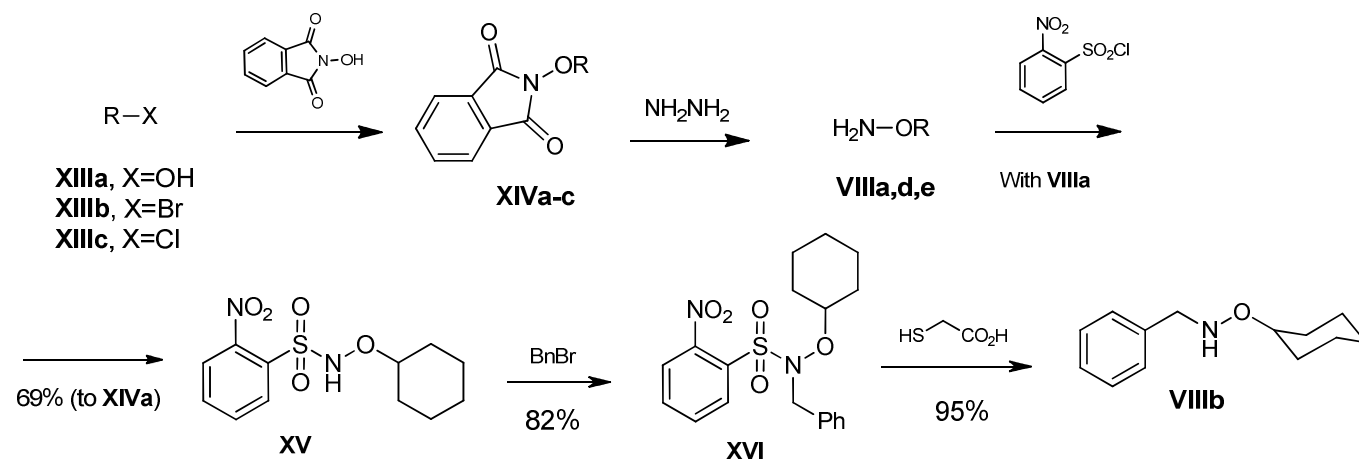


53
54
55
56
57
58
59
60

The hydroxylamine intermediates **VIIIa,b,d,e** of carboxamide amines **IV** and sulfonamide amines **V** were synthesized starting from 2-hydroxyisoindoline-1,3-dione which was alkylated with cyclohexyl alcohol **XIIIa** upon *Mitsunobu* conditions, with cyclohexylmethyl bromide **XIIIb** in the presence of

K_2CO_3 in DMSO, or with 2-(4-morpholinyl)ethyl chloride (**XIIIc**) in the presence of 1,8-diazabicyclo[5.4.0]undec-7-ene (DBU) to give the *O*-substituted derivatives **XIVa-c**. Removal of the phthalimide protective group of compounds **XIVa-c** gave *O*-hydroxylamine derivatives **VIIIa**, **VIII d**, and **VIII e**, respectively. Compound **VIII a** was further converted into *N*-monobenzyl derivative **VIII b** via 2-nitrobenzosulfonamide intermediates **XV** and **XVI** (Scheme 6).

Scheme 6. Preparation of Hydroxylamines **VIII a,b,d,e**



No	R
XIII a , XIV a , VIII a	Cyclohexyl
XIII b , XIV b , VIII d	cyclohexylmethyl
XIII c , XIV c , VIII e	2-(4-morpholinyl)ethyl

Another series of *N,O*-disubstituted hydroxylamines **VIII c,f-i** were prepared from cyclic ketones

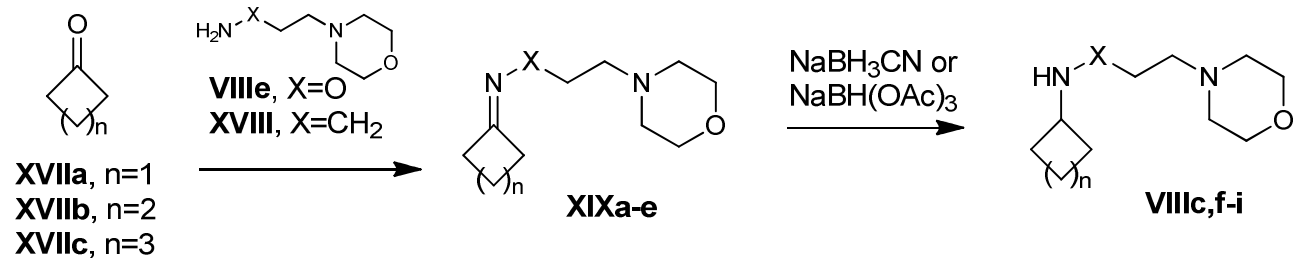
XVII a-c and *O*-(2-morpholinoethyl)hydroxylamine (**VIII e**) or 3-morpholinopropan-1-amine (**XVIII**)

by reductive amination (Scheme 7). Condensation of the ketones **XVII a-c** with the amino compounds

VIII e or **XVIII** gave the corresponding intermediate oximes or imines **XIX a-e**, which were reduced to

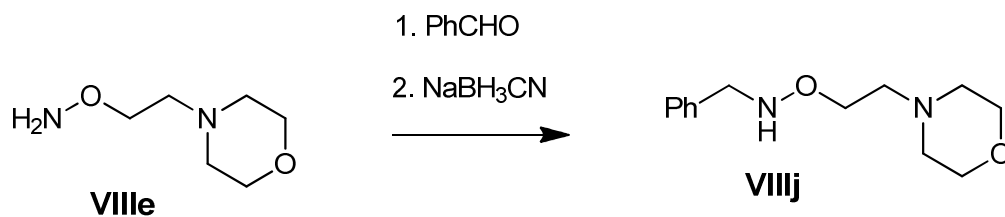
saturated structures **VIII c,f-i**.

Scheme 7. Preparation of Hydroxylamines VIIIc,f,h and Amines VIIIg,i



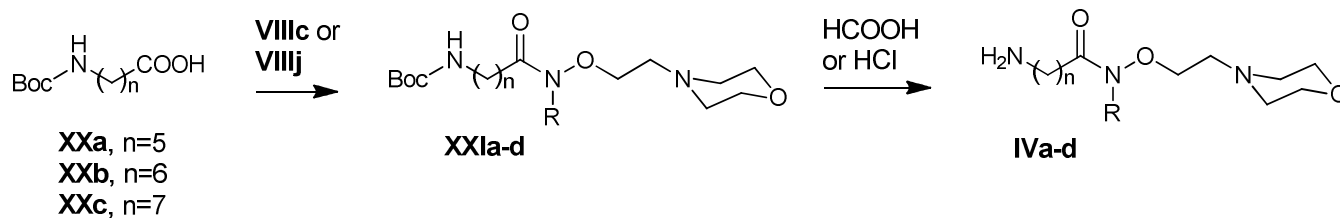
No	n	X
XIXa, VIIIIf	1	O
XIXb, VIIIIg	1	CH ₂
XIXc, VIIIHh	2	O
XIXd, VIIIc	3	O
XIXe, VIIIi	3	CH ₂

By a similar one-pot reductive amination protocol *O*-(2-morpholinoethyl)hydroxylamine (**VIIIe**) and benzaldehyde afforded *N*-benzyl-*O*-(2-morpholinoethyl)hydroxylamine (**VIIIj**) (Scheme 8).

Scheme 8. Synthesis of *N*-Benzyl-*O*-(2-morpholinoethyl)hydroxylamine (**VIIIj**)

The hydroxamate amines **IVa-d** were prepared from *N*-Boc protected ω -amino hexanoic, heptanoic, and octanoic acids **XXa-c** which were condensed with hydroxylamine **VIIIj** in the presence of EDC or with hydroxylamine **VIIIc** in the presence of HATU to afford the corresponding hydroxamates **XXIa-d** which were deprotected to obtain compounds **IVa-d** (Scheme 9).

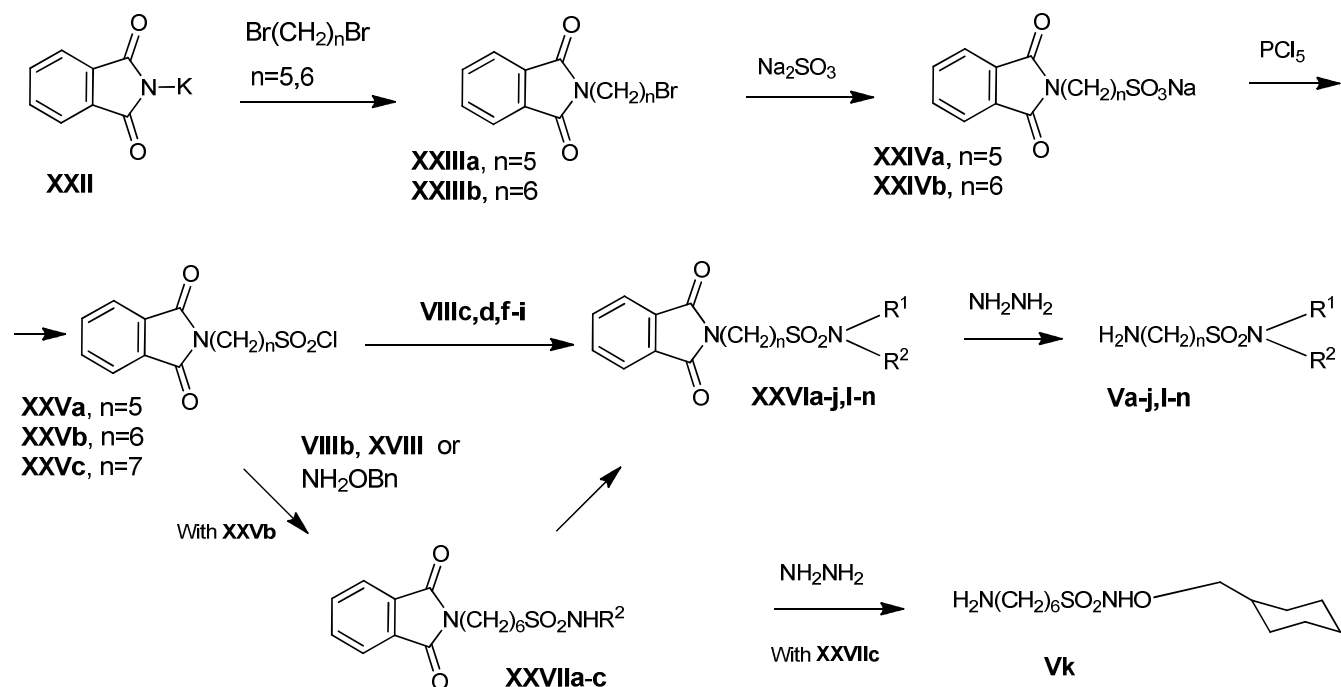
Scheme 9. Synthesis of Hydroxamate Amines IVa-d



No	n	R
XXIa, IVa	5	Bn
XXIb, IVb	6	Cyclohexyl
XXIc, IVc	7	Bn
XXId, IVd	6	Bn

The synthesis of sulfonamide amines **Va-n** was based on the condensation of phthalyl-protected ω-aminopentane, aminohexane, and aminoheptane sulfonyl chlorides **XXVa-c** with appropriate amine or hydroxylamine derivatives to produce the corresponding sulfonamides **XXVIa-j,l-n** (Scheme 10). In the case of tertiary sulfonamides **XXVIh,i,l,m** the synthesis included an extra alkylation step of initially obtained secondary sulfonamides **XXVIIa-c**. The following treatment of the sulfonamides **XXVIa-j,l-n** and **XXVIIc** with hydrazine produced the sulfonamide amines **Va-n**. The intermediate sulfonyl chlorides **XXVa,b** were obtained by a short synthetic sequence from potassium phthalimide **XXII**, including mono-alkylation of the latter with 1,5-dibromopentane or 1,6-dibromohexane, treatment of the obtained bromo derivatives **XXIIIa,b** with sodium sulfite and conversion of the resulting sodium sulfonates **XXIVa,b** into the corresponding sulfonyl chlorides **XXVa,b** with PCl_5 . The sulfonyl chloride **XXVc** was obtained using literature procedure.⁴⁰

Scheme 10. Synthesis of Sulfonamide Amines Va-n



No	n	R ¹	R ²	No	n	R ¹	R ²
XXVIa, Va	5			XXVIIb, XXVIIh, Vh	6		
XXVIb, Vb	5			XXVIIc, XXVIIi, Vi	6		
XXVIc, Vc	6			XXVIj, Vj	7		
XXVId, Vd	6			XXVIIa, XXVII, VI	6		
XXVIe, Ve	6			XXVIIc, XXVIIm, Vm	6		
XXVIf, Vf	6			XXVIIl, Vn	5		
XXVIg, Vg	6						

SAR

Compound **1** and **2** (Figure 1) represent two distinct compound classes, which are bioisosters, both targeting the NAMPT enzyme. The common features in the two compounds are the pyridyl head-group, a functional group with hydrogen binding capabilities, a linker chain and an aromatic group in the end of the linker. With the aim of discovering new compounds with improved activity and toxicological properties the SAR of these compounds was explored by modification of the mentioned key structural elements (Figure 2).

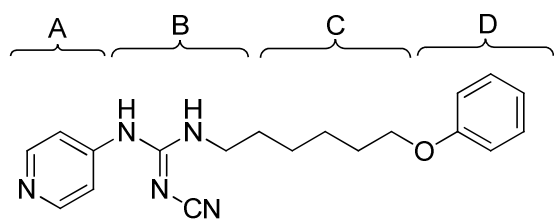


Figure 2. Overview of the sequence of the described SAR work: 1) Modification of aromatic end group D to hydroxamic acid esters (compounds **4-12**). 2) SAR for pyridyl head group A (comp. **10, 13**). 3) SAR of hydrogen binding group B, replacement of cyanoguanidine with squaric acid and urea (comp. **26, 28, 29, 38** and **39**). 4) Change of the hydroxamic acid ester for a preferred alkoxy sulphonamide or sulphonamide in D (e.g. **10** vs. **15, 26** vs. **31**). 5) Optimisation of linker length C and end group for squaric acids (**31-34** and **36**) and urea derivatives (**40-42** and **44**). 6) Final optimisation of the cyanoguanidine series with a pyridyl head-group and an alkoxy sulphoneamide (comp. **17** and **20-25**).

The primary determination of activity was performed using a WST-1 cell viability and proliferation assay in two cell lines, a breast cancer, MCF-7, and an ovarian carcinoma, A2780, cell line. The WST-1 assay determines the metabolic activity of the cells, in a process dependent on NADH as coenzyme, thus this assay will have a strong functional connection to the NAMPT inhibition.

Modification of aromatic end group

Initially, the aromatic end group of compound **2** was modified by preparing novel hydroxamic acid esters which immediately gave potent analogues in the in vitro test system, represented by the first hit compound **4** with nanomolar activity (Table 1 and Figure 3).

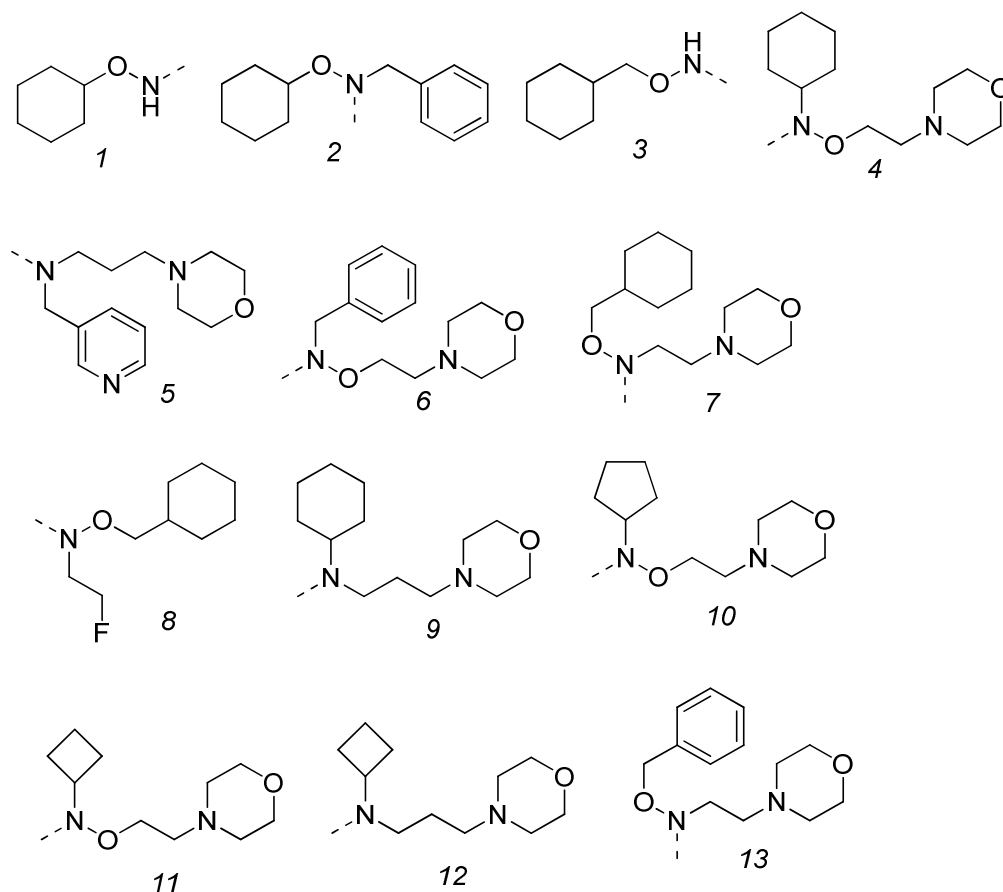
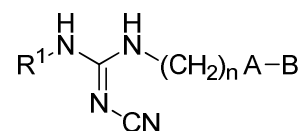


Figure 3. Structures of molecular fragment B in Table 1, 3 and 4.

Table 1. NAMPT inhibitors with a cyanoguanidine binding group



Cell line	A2780 ^a						MCF-7 ^a	
Compound	R ¹	n	A	B ^b structure	IC ₅₀ , (mean, nM)	SD	IC ₅₀ , (mean, nM)	SD

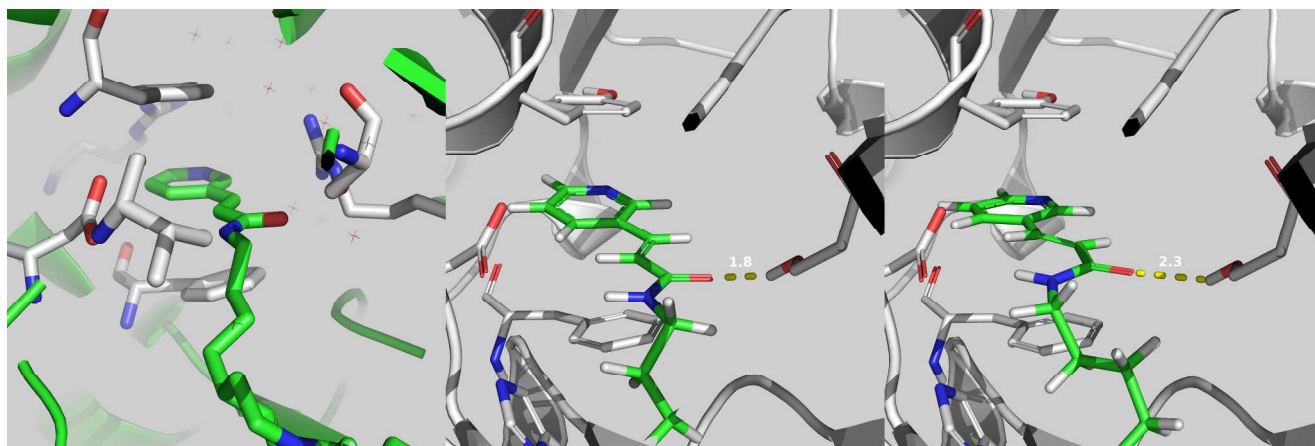
1	1, APO866	-	-	-	-	1.6	±1.5	7.4	±0.68
2	2, CHS828	-	-	-	-	0.56	±0.19	1.6	±1.3
3	4	4-pyridyl	6	CO	1	35	±13	940	±377
4	5	4-pyridyl	6	CO	2	0.055	±0.036	1	±0.80
5	10	4-pyridyl	6	CO	4	0.1	±0.11	0.42	±0.08
6	11	4-pyridyl	7	CO	6	0.01	±0.014	ND ^c	
7	12	4-pyridyl	5	CO	6	0.081	±0.10	0.021	±0.002
8	13	phenyl	6	CO	4	98	±34	1016	±737
9	14	4-pyridyl	6	SO ₂	3	0.16	±0.18	3.4	±2.3
10	15	4-pyridyl	6	SO ₂	4	0.025	±0.021	0.33	±0.63
11	16	3-pyridyl	6	SO ₂	4	0.51	±0.31	2.9	±1.10
12	17	4-pyridyl	6	SO ₂	8	0.052	±0.060	0.1	±0.19
13	18	4-pyridyl	6	SO ₂	9	0.16	±0.35	0.11	±0.24
14	19	4-pyridyl	7	SO ₂	4	0.089	±0.091	0.29	±0.42
15	20	4-pyridyl	5	SO ₂	4	0.011	±0.017	0.036	±0.015
16	21	4-pyridyl	6	SO ₂	10	0.0041	±0.0032	ND ^c	
17	22	4-pyridyl	6	SO ₂	11	0.049	±0.031	0.007	±0.008
18	23	4-pyridyl	6	SO ₂	12	0.091	±0.11	0.1	±0.01
19	24	4-pyridyl	5	SO ₂	10	0.022	±0.03	0.041	±0.01
20	25	4-pyridyl	6	SO ₂	13	0.053	±0.07	0.63	±0.29

^a Activities were determined in a WST-1 assay. ^b See Figure 3. ^c ND, not determined.

In the crystal structure of NAMPT co-crystallized with compound **1** a rather large binding region near the surface of the protein can be observed where the side chain end group of the ligand is placed.^{41,42} As in earlier work the published crystal structure of NAMPT co-crystallized with **1** was used as starting point for docking analysis.⁴³ (PDB ID 2GVJ) which was carried out in Glide (further details in Experimentals). Previously, we found that different ligands for NAMPT had such similar geometric features that compound **2** and **5** could even be docked into the crystal structure of compound **1** *without* removing the crystallographic water molecules in the active site.⁴³ However, due to the much larger and more diverse set of ligands we chose to completely remove the crystallographic waters in the current study. In the supporting information we have included additional pictures showing the crystal structure

1 with the crystallographic water molecules present and it is evident that only few water molecules
2 penetrate the active site when the ligand is present.
3
4
5
6

7 When **1** was re-docked into the empty active it achieved the crucial hydrogen bonding to Ser275, albeit
8 with a slightly longer distance (2.3Å) compared to the 1.8Å observed in the X-ray structure (Figure 4).
9
10
11
12
13



14
15
16
17
18
19
20
21
22
23
24
25
26
27
28
29
30
31
32 **Figure 4.** Left: Illustration of **1** docked in the NAMPT X-ray structure (PDB id 2GVJ). Notice the lack
33 of crystallographic waters in the binding cleft (additional orientations are included in the Supporting
34 Information). Center: The pose of **1** observed in the X-ray with hydrogens added and waters removed.
35
36 Right: The pose obtained by docking **1** into the “dry” active site of NAMPT.
37
38
39
40
41
42
43

44 Docking of compound **4** suggested a similar binding mode as compared to **1** (Figure 5) where the
45 cyanoguanidine is capable of achieving a similar hydrogen bond to Ser275. Furthermore, the
46 cyanoguanidine established two new hydrogen bonds to Asp219, which may serve as part of the
47 explanation for the efficiency of this chemical motif.
48
49
50
51
52
53
54
55
56
57
58
59
60

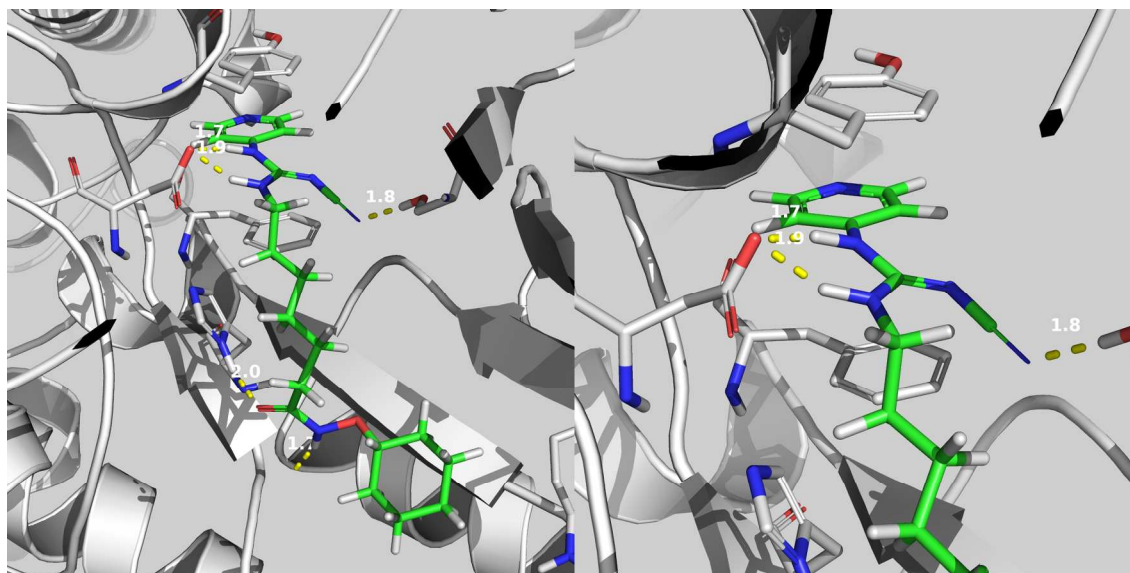
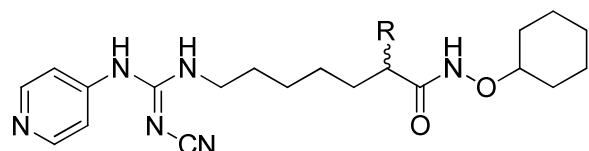


Figure 5. Left: The conformation of **4** docked into the NAMPT active site (PDB id 2GVJ). Right: Close-up of the pyridine sandwich with the three hydrogen bonds made by the cyanoguanidine moiety.

To investigate the preferred binding orientation of the side chain in compound **4** the close alpha-methyl and alpha-benzyl analogues were prepared in an enantiomerically pure form. A stereochemical preference for the (*S*)-methyl derivative (**6**) was found, with a 40 times higher activity, as compared with the (*R*)-methyl derivative (**7**) (Table 2). However, this was not reflected in the calculated docking scores for the interaction which showed a reversed preference. The reasons for this discrepancy were not clear from visual inspection of the docked structures since they were virtually superimposable in spite of the difference in stereochemistry. Therefore we speculate that the observed difference in activity could be due to one of several factors that are not accounted for in simple docking calculations such as protein flexibility or different interactions with the hydrogen-bond network between enzyme and water molecules. The similarity in physico-chemical properties leads us to believe that the observed difference in not due to differences in pharmacokinetics. The activity difference was very small for the corresponding benzyl enantiomers (**8**, **9**), probably due to the similar size of the binding end-groups in the molecule (Table 2). Thus, the docking analysis of these structures did not reveal any obvious

differences, or a preferred fit, of the enantiomers with the protein structure. Even though the chiral derivatives were very potent with sub-nanomolar activity this compound group was not further explored due to a generally low stability and rapid hydrolysis in mouse plasma (data not shown).

Table 2. NAMPT inhibitors with a chiral end group



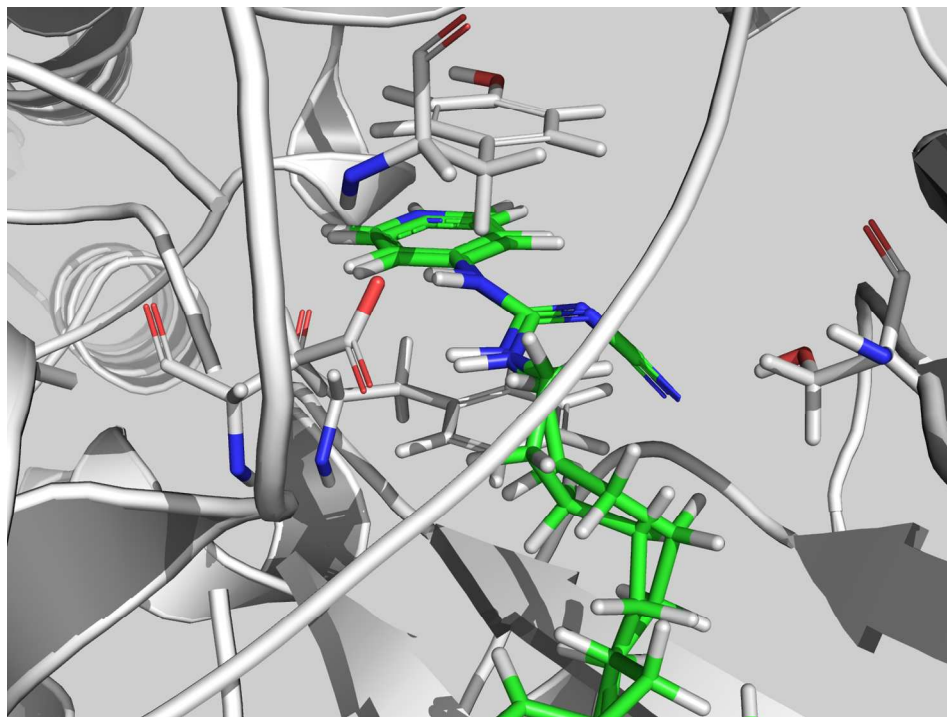
Cell line	A2780 ^a		MCF-7 ^a		
Compound	R	IC ₅₀ , (nM)	SD	IC ₅₀ , (nM)	SD
6	(S)-Me	0.08	ND ^b	1	±0.8
7	(R)-Me	3.9	±0.64	38.3	±27.8
8	(S)-Bn	0.32	±0.03	5.3	±3.4
9	(R)-Bn	0.22	±0.28	1.7	±0.6

^a Activities were determined in a WST-1 assay. ^b ND, not determined.

An improvement of both stability and activity was found for the hydroxamic acid esters bearing an additional substituent on the hydroxamic acid nitrogen, compounds **5**, **10**, **11** and **12** all exhibiting sub-nM activities (Table 1). From the docked structures it is clear that these ligands are capable of spanning the wide entrance of the cleft of the protein active site thereby increasing their binding affinities. At present time it is unclear whether this increase is due to additional (non-specific) binding interactions with the protein surface or that the increased binding is caused by a decreased number of accessible conformations of the free ligands.

SAR for pyridyl head group

1 In earlier studies the pyridyl head-group in the parent compounds has been found essential for high
2 activity.²² To investigate the importance of the head-group in this series a phenyl derivative, compound
3 **13**, was prepared and found approx. 1000-2000 times less potent as compared with the analogous
4 **13**, was prepared and found approx. 1000-2000 times less potent as compared with the analogous
5 **13**, was prepared and found approx. 1000-2000 times less potent as compared with the analogous
6 **13**, was prepared and found approx. 1000-2000 times less potent as compared with the analogous
7 compound **10** (Table 1). This large difference in activity is difficult to explain since the two head-groups
8 (phenyl and pyridine) are both capable of sandwiching between Tyr18 and Phe193 (Figure 6).
9
10
11
12
13



14
15
16
17
18
19
20
21
22
23
24
25
26
27
28
29
30
31
32
33
34
35
36
37
38
39
40
41 **Figure 6.** Docking of **10** and **13** in the NAMPT X-ray structure (PDB id 2GVJ), where it is clear that
42 the head groups are virtually superimposable.
43
44
45
46
47

48 To investigate this difference in more detail we carried out an analysis of the binding energy using
49 density functional theory (DFT) in combination with the B3LYP functional with added dispersion
50 corrections (DFT-d3).
51
52
53
54
55
56
57
58
59
60

1 Due to the computational demands of DFT-d3 the enzyme was reduced to an active site model
2 consisting of Arg-196, B-chain Tyr-18, B-chain Asp-16, Asp 219, Phe-193, Arg-311, and Ser-275. The
3 amino acids were truncated at the C α in line with earlier work.⁴⁴ Since the aim of the study was
4 primarily to delineate the effect of the head group it was also decided to truncate the ligands in the
5 spacer region so it consisted of just a single methyl group. A single-point energy calculation shows that
6 the pyridine has an interaction energy that is 22 kJ/mol larger than for the corresponding structure with a
7 phenyl as head-group, which is in qualitative agreement with the experimental results. In the
8 cyanoguanidine series also the 4-pyridyl head group was compared with the analogues 3-pyridyl
9 derivative, compound **15** vs. **16** (Table 1). This comparison showed a >10 fold activity preference for
10 the 4-pyridyl group. A similar activity preference was found for other 4-pyridyl versus 3-pyridyl
11 compound pairs (data not shown), but in this case the observation could not be explained by the DFT
12 calculations since 4-pyridyl and 3-pyridyl head groups had a similar stabilization energy (within 1
13 kJ/mol). At present it is unclear whether more extended conformational sampling combined with e.g.
14 advanced mixed quantum mechanics/molecular mechanics (QM/MM) calculations could delineate this
15 interesting experimental difference in activity.
16
17
18
19
20
21
22
23
24
25
26
27
28
29
30
31
32
33
34
35
36
37

38 *SAR of hydrogen binding group*

39 The next structural modification made was a replacement of the cyanoguanidine with other hydrogen
40 binding groups. There have been previous attempts to substitute the cyanoguanidine or amide group of
41 compounds **1** and **2** with other groups retaining activity (Figure 1).²⁸ In this investigation the most
42 promising substitutions were found to be the squaric acid and urea analogues. The squaric acid
43 compounds **26**, **28**, **29** (Table 3) and the urea and thiourea derivatives with a 3-picolyl head group,
44 compounds **38** and **39** respectively (Table 4), both series with a hydroxamic acid ester end group, all
45 were potent inhibitors of proliferation. As expected, docking of these structures showed that they too
46 were capable of obtaining the crucial hydrogen-bonding interactions in the active site of NAMPT
47 (Figure 7).
48
49
50
51
52
53
54
55
56
57
58
59
60

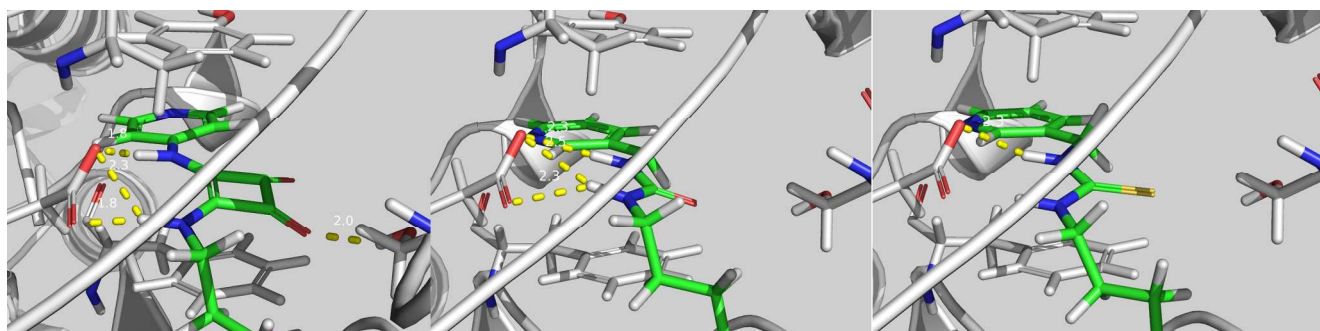
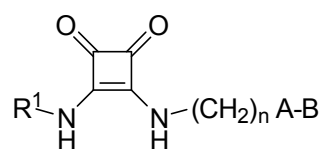


Figure 7. Compounds docked in the NAMPT X-ray structure (PDB id 2GVJ). Left: **26**, a representative of the squaric acid series with dotted lines indicating the hydrogen bonds made to Ser275 and Asp219. Center: **38**, the urea linker also allows hydrogen bonds to be made to Asp219. Right: **39**, also the larger thiourea can be accommodated in the active site.

Squaric acids with similar side chains as the parent compounds **1** and **2** have been reported in the patent literature to have anti-proliferative activity.⁴⁵ This finding suggests a further exploration of the squaric acid bioisosters with novel side chains.

Table 3. NAMPT inhibitors with a squaric acid binding group

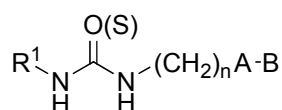


Cell line					A2780 ^a		MCF-7 ^a	
Compound	R ¹	n	A	B ^b structure	IC ₅₀ , (mean, nM)	SD	IC ₅₀ , mean, (nM)	SD
26	4-pyridyl	6	CO	4	0.03	±0.02	ND ^c	
27	4-pyridyl	6	SO ₂	5	4.1	±2.2	21.6	±4.5

28	4-pyridyl	6	CO	6	0.29	±0.32	12.3	±5.0
29	4-pyridyl	5	CO	6	0.68	±0.47	23	±1.1
30	4-pyridyl	6	SO ₂	7	0.73	±0.03	10.8	±2.3
31	4-pyridyl	6	SO ₂	4	0.49	±0.22	9	±2.9
32	4-pyridyl	7	SO ₂	4	0.49	±0.17	8	±5.2
33	4-pyridyl	5	SO ₂	4	0.57	±0.12	35.8	±8.4
34	4-pyridyl	6	SO ₂	10	0.59	±0.35	13.7	±2.4
35	4-pyridyl	6	SO ₂	11	0.2	±0.14	29.1	±6.4
36	4-pyridyl	5	SO ₂	10	0.38	±0.05	46.3	±6.3

^a Activities were determined in a WST-1 assay. ^b See Figure 3. ^c ND, not determined

Table 4. NAMPT inhibitors with a urea (thiourea) binding group



Cell line					A2780 ^a		MCF-7 ^a	
Compound	R ¹	n	A	B ^b structure	IC ₅₀ , (mean, nM)	SD	IC ₅₀ , (mean, nM)	SD
37	4-pyridyl	6	SO ₂	4	0.25	±0.13	0.05	±0.01
38	3-picolyl	6	CO	4	0.27	±0.13	0.37	±0.51
39	3-picolyl ^c	6	CO	4	0.91	±0.31	5.5	±2.2
40	4-pyridyl	6	SO ₂	7	0.56	±0.01	1.4	±0.05
41	3-picolyl	6	SO ₂	7	0.17	±0.06	0.93	±0.11
42	4-pyridyl	5	SO ₂	4	3.4	±2.2	28	±11.2

1	43	4-pyridyl	7	SO ₂	4	1.8	±0.07	7.4	±4.6
2									
3	44	3-picolyl	5	SO ₂	4	4.6	±4.5	6.5	±5.7
4									
5	45	3-picolyl	7	SO ₂	4	0.31	±0.11	3.6	±2.3
6									
7	46	3-picolyl	6	SO ₂	10	0.58	±0.18	5.8	±0.15
8									
9									
10	47	3-picolyl	6	SO ₂	11	2.2	±0.12	11	±5.0
11									
12	48	3-picolyl	6	SO ₂	12	1.7	±0.21	8.7	±7.2
13									
14	49	3-picolyl	5	SO ₂	11	13	±6.4	49	±33.7
15									
16									
17	50	3-picolyl	5	SO ₂	10	2.7	±1.9	7	±1.2
18									
19	51	4-pyridyl ^c	6	SO ₂	10	0.16	±0.15	0.31	±0.40

^a Activities were determined in a WST-1 assay. ^b See Figure 3. ^c The compound is a thiourea.

Change of the hydroxamic acid ester

With three structural core elements, the cyanoguanidine, the squaric acid and the urea, all producing highly active compounds, in hand a further optimization was structured. Changing the hydroxamic acid ester for an alkoxy sulphonamide or sulphonamide gave a more robust series of compounds with high activity and this substitution was used in the further SAR work (see e.g. **10** vs. **15**, Table 1 and **26** vs. **31**, Table 3).

Squaric acid series

In the squaric acid series, compounds **31**, **34**, and **35** were prepared to explore the effect of ring size in the end group, however, no significant difference in binding affinity/anti-proliferative activity was found (Table 3). This is understandable also from the docking results since the head groups dock in a similar position in the active site, as expected (Figure 8 left), whereas the flexible end of the chain can freely position itself in the wide entrance region of the catalytic cleft.

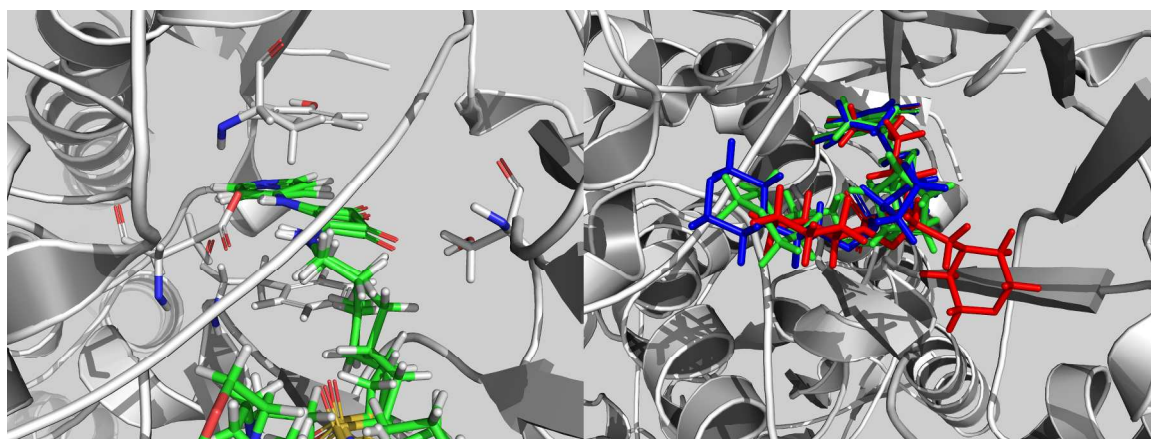


Figure 8. Compounds docked in the NAMPT X-ray structure (PDB id 2GVJ). Left: Compounds **31**, **34**, and **35** all dock into the sandwich region of the enzyme. Right: The wide entrance region allows the ligands to obtain different positions that do not offer any differences in activity between compounds having a 5-membered (green), 6-membered (red), or 4-membered ring (blue) as substituent on nitrogen.

Likewise the linker length was varied from 5-7 carbons in compounds **31-33** and **34** vs. **36** which gave compounds with similar activity, however, with a slight activity preference for compounds with 6 carbons in the linker (Table 3). Shorter and longer linker chains gave compounds with lower anti-proliferative activity (data not shown).

For compounds **31-33** the docking analysis shows a preference for a hydrogen bond interaction between the sulphonamide moiety and His191. This enforces a constraint on the length between the sulphonamide and the pyridine head-group, which is suitable for a 6-carbon linker (**31**). The docking results showed that the shorter chain introduces strain in the structure (**33**) and the longer 7-carbon linker has to coil up to satisfy the distance requirement (**32**). However, we should stress that the similarity in the biological activity shows that such accommodation is possible and indeed takes place without significant loss in activity.

1 The squaric acid **27**, a sulphone amide, was less active, however, this compound was not strictly
2 analogous to any alkoxy sulphone amide since it has an additional pyridine group in the end group of
3 the molecule. In all three series the sulphonamide end groups were found equipotent or slightly less
4 potent as compared with similar alkoxy sulphonamide (see compounds **18**, **23**, **27** and **48**, Table 1-4).
5
6
7
8
9

10 11 *Urea series*

12 The urea derivatives were designed as analogues to compound **1** where the unsaturated amide was
13 replaced by a urea group. In this series, compounds with a 4-pyridyl or a 3-picolyl head-group were
14 compared, compounds **40** vs. **41** and **42** vs. **44**, and found equipotent despite the structural difference in
15 the head group (Table 4). Computational modeling of these interactions showed that despite the
16 difference in the location of the pyridine nitrogen the aromatic group positions itself perfectly aligned in
17 the pocket between Tyr18 and Phe193. This introduces a slight difference in the orientation of the urea
18 moiety, but does not hinder the formation of hydrogen bonds to Asp219. As mentioned earlier, our
19 simple DFT model of the binding site does not reveal any differences in the π - π stacking ability of the
20 two head groups which is in line with the observation for the urea series.
21
22
23
24
25
26
27
28
29
30
31
32
33
34
35
36
37

38 Similar to the squaric acid analogues a linker of 5-6 carbons gave highly active compounds both with a
39 pyridyl head-group (**37**, **42**, **43**) and a picolyl head-group (**46**, **47**, **49**, **50**, Table 4).
40
41
42

43 Also in the urea series many of the analogues showed sub nM activities either with a pyridyl or picolyl
44 head-group, a urea or thio-urea binding group and a series of different end groupings.
45
46
47
48

49 *Cyanoguanidine series*

50 Returning to the cyanoguanidine series with a pyridyl head-group and an alkoxy sulphone amide
51 connecting the linker and end groups the most potent compounds with low pM anti-proliferative
52 activity, e.g. compounds **17** and **20-25**, were found (Table 1). Similar to the other series a linker of 6
53 carbons was optimal.
54
55
56
57
58
59
60

In summary, using a functional cell proliferation assay a rather broad SAR was determined. Highly active compounds were found in all three series, the cyanoguanidine, the squaric acid and the urea series, suggesting an analogous interaction with the target NAMPT enzyme. Also, a similar substitution pattern was used to obtain the most potent compounds in the three series suggesting a similar binding to the target.

In vitro activity and mode of action.

To further characterize the key compounds, the IC₅₀ values of a number of them were established in the colon cancer cell line HCT-116 and a derived compound **1** resistant cell line HCT-116/APO866 (Table 5). Determination of the actual sensitivity of the cell line with acquired resistance was not possible.

However, the resistance towards the compounds was at least 128-2632 fold higher in HCT-116/APO866 compared to the parental cell line. The mechanism of resistance in HCT-116/APO866 has been determined to be specifically due to a mutation, H191R, in the active site of NAMPT which results in highly specific resistance.^{29,43} Thus, the high level of cross-resistance observed for the compounds in this study strongly suggests that their mechanism of action likewise is through inhibiting NAMPT and thus similar to that of compound **1**.

Table 5. IC₅₀ values for key compounds for anti-proliferative effects in HCT-116 and compound **1 resistant HCT-116/APO cells**

Cell line	HCT-116 ^a		HCT-116/APO866 ^a
Compound	IC ₅₀ (nM)	±SD	IC ₅₀ (nM)
1	10.9	6.1	946
15	1,9	0,2	>5000
17	3,6	2,4	>5000
31	39	13	>5000
37	5,3	2,9	>5000

^a Activities were determined in a WST-1 assay.

In order to confirm the on-target mechanism of action for the new series of compounds the enzyme inhibitory activity was determined using a NAMPT enzymatic assay with HepG2 lysates as source of NAMPT enzyme (Table 6). Even though the correlation with the anti-proliferative activity data was not perfect, all tested compounds showed high potency with low nM activity, thus a strong support for a direct enzyme interaction. The discrepancy between enzyme inhibition and anti-proliferative activity is suggested to be due to the different properties of the compounds such as cell penetration which is important in the cellular assay. Compounds were selected for further testing primarily based on in vitro activity but also to cover the chemical classes. Key compounds were also characterised in a clonogenic assay in several cancer cell lines (Table 7). Compounds **15** and **17** showed similar or increased potency in these assays as compared to reference compound **1** and were thus selected for further in vivo characterization.

Table 6. NAMPT enzyme assay (IC₅₀, nM)

Comp nr	1	2	4	5	10	11	14	15	17
IC ₅₀ (nM)	2.2	18.3	1.1	38.5	0.2	4.4	2.4	0.3	3.2

Comp nr	18	27	32	33	37	39	40	41
IC ₅₀ (nM)	2.4	22.8	3.6	49.6	49	8.2	133.2	11.8

Table 7. Clonogenic assay for compounds **15, **17** and **1** in a selection of cancer cell lines**

Compound, Cell line	15 , IC ₅₀ (nM)	17 , IC ₅₀ (nM)	1 , IC ₅₀ (nM)
A2780	0.55 (24h)	0.43 (16h)	5.7
A431	>50	ND ^a	6.1
DU145	>50	6.39	ND ^a

MCF-7	>50 (24h) 1.9 (96 h)	>50 (24h) 0.98 (96 h)	8.4 ND ^a
NYH	0.3	0.05	1.5
PC-3	0.53	0.35	3.8
SK-OV-3	9.9	3.4	211

^a ND, not determined

In vivo antitumour activity.

Compounds with potent (nM) activity from all series were taken forward to tests of pharmacokinetics and preliminary toxicology effects in mouse as a selection filter for in vivo test in an A2780 xenograft mouse model (Table 8). Several of the new compounds compared well with the reference compound **1** and based on these data compounds were selected. Most compounds in these series exhibited a relatively short half-life, approximately 20 min, but with an adequate systemic exposure (AUC). Therefore, in this early screen for pharmacological activity in vivo the compounds were administered i.p. to secure a sufficient exposure of the compound in the animal.

Table 8. Toxicological and pharmacokinetic data for selected derivatives as determined in mouse

Compound	Toxicology ^a			Pharmacokinetics					
	MTD (mg/kg)	Dose for PK (mg/kg)	Route	T _{1/2} (hrs)	T _{max} (hrs)	C _{max} (ng/ml)	V _z (ml/kg)	CL (ml/hr/kg)	AUC (hr*ng/ml)
1	10<MTD<50	20	i.v.	0.4	0.25	14563	998	1620	12337
15	MTD<10	50	i.v.	0.18	0.08	14102	1275	4906	10184
17	10<MTD<50	50	i.v.	0.36	0.08	78519	547	1052	47514
31	10<MTD<50	50	i.v.	0.21	0.083	33535	1200	3995	12499
37	MTD<10	50	i.v.	0.45	0.08	14827	4600	7105	7018

^a The compound toxicity (MTD) was estimated in NMRI mice dosing the compounds bid i.p. for 5 consecutive days, determining weight loss and blood cell counts.

Treatment with compound **17** (15 mg/kg bid i.p. for 10 consecutive days (small tumours) or two 5 day cycles (large tumours) had good therapeutic effect in both small and large A2780 tumours (Figure 9). A clear decrease was seen in the tumour volumes during the treatment period, some mice even showed a transient cure and eradication of the tumour. After treatment, the tumours resumed growth at various time points, and grew to the maximum allowed size (1000 mm³). Treatment with compound **17**, 15 mg/kg, using the schedules above was well tolerated and did not affect the body weight as compared with vehicle treated animals (Figure 9, insert).

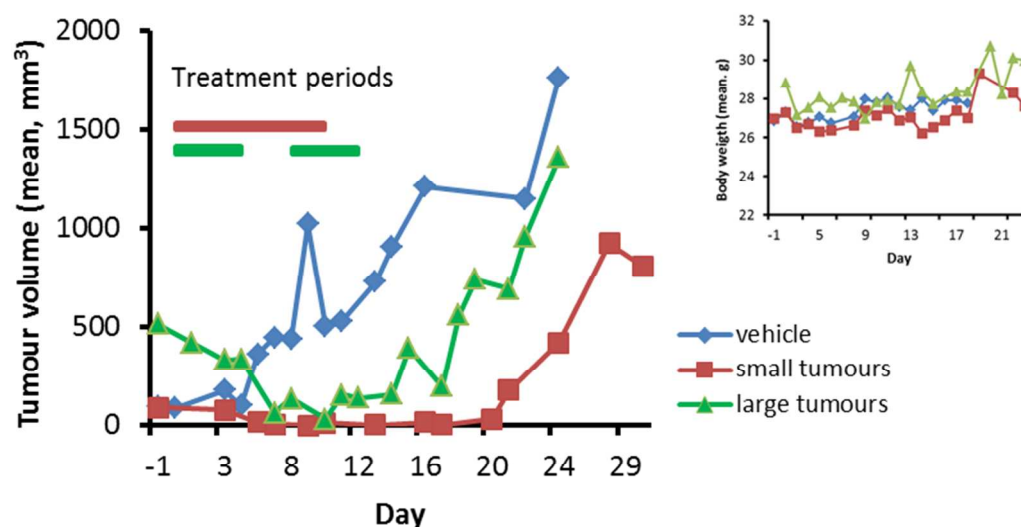
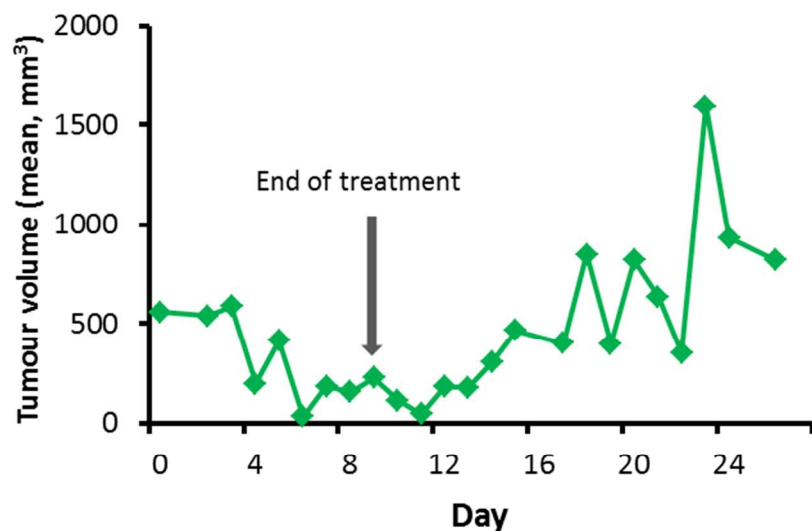


Figure 9. Tumour growth curves of compound **17** in an A2780 xenograft mouse model. (15 mg/kg bid i.p. on days 0-4 + 7-11 (large tumours; starting volume 500 mm³) or days 0-9 (small tumours; starting volume 100 mm³). Inserted graph; body weight change during treatment.

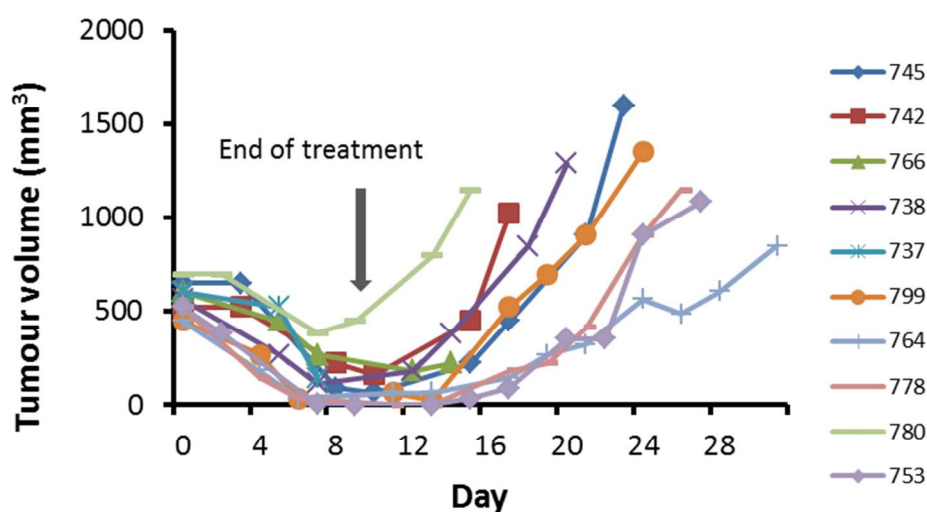
Similarly, compound **15** was tested in the A2780 xenograft model with large tumours (3 mg/kg, i.p., bid, 10 consecutive days) (Figure 10). This compound (**15**) showed good efficacy and on average, treatment reduced the tumour volume significantly to one fifth of the volume from start of treatment (Figure 10A). This dose was found well tolerated in the mice (Figure 10C). Compound **15** was tested at higher

1 doses (5 and 10 mg/kg) with very clear therapeutic effects, however already at 5 mg/kg four of nine
2 mice showed toxic signs in form of body weight loss and reduced activity level as compared to control
3 mice showed toxic signs in form of body weight loss and reduced activity level as compared to control
4 which was further accentuated at 10 mg/kg (data not shown). Thus, it was concluded that a 3 mg/kg bid
5 dose was at the MTD level for compound **15**, in this model.
6
7
8
9
10
11
12
13

A



B



C

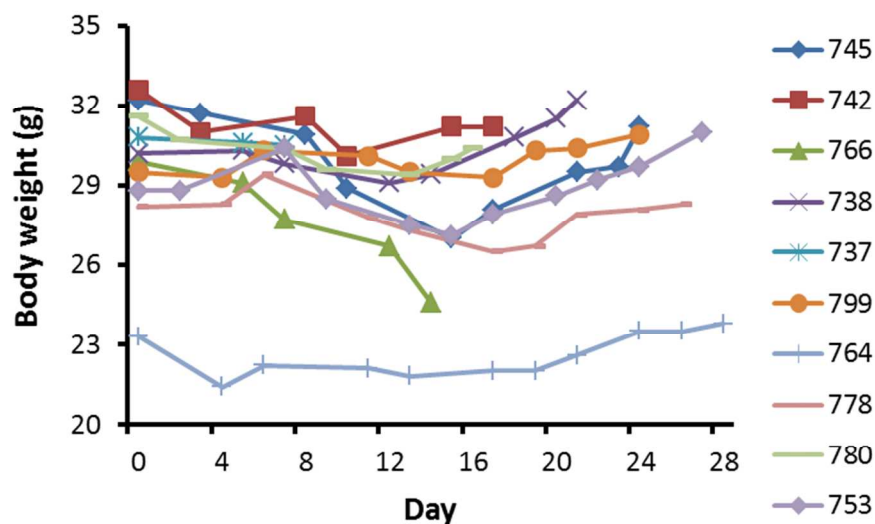
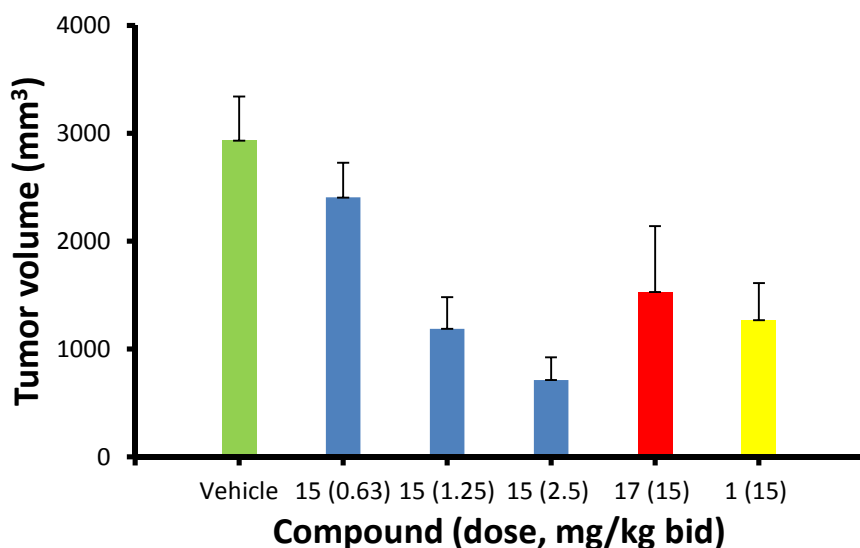


Figure 10. Treatment with compound **15**, in an A2780 xenograft mouse model (large tumours, 3 mg/kg, i.p., bid). A) Mean tumour volume. B) Tumour volume in individual mice C) Body weight during treatment in individual mice.

In a comparative study with these two compounds (**15** and **17**) and the reference compound **1**, compound **15** was found approximately 12 times more potent than **1** in the A2780 xenograft mouse model (schedule; i.p. bid day 0-4, starting tumour volume 100 mm³) as measured by the tumour volume at day 14. Significant reduction of A2780 tumour volume at day 14 was observed after treatment with compound **15**, 1.25 and 2.5 mg/kg and compound **1**, 15 mg/kg. Dose response effect of **15**, 0.63, 1.25 and 2.5 mg/kg was observed with percent volume of treated tumours versus control T/C% of 82, 40 and 24%, respectively. Also, some effect (T/C=52%), however not significant, was determined after

1 treatment with compound **17** and compound **1** (Figure 11). Critical body weight losses were not
2
3 observed in any treatment groups.

4
5
6 In summary, in vivo the selected compounds showed an equal or increased potency as compared with
7
8 reference compound **1**, with no critical signs of toxicology using effective doses. These highly
9
10 promising results suggest a continuation of studies of this compound class.
11



12
13
14
15
16
17
18
19
20
21
22
23
24
25
26
27
28
29
30
31
32
33
34
35
36
37
38 **Figure 11.** Tumour volume at day 14 after treatment with compounds **15** (0.63, 1.25, 2.5 mg/kg), **17** (15
39 mg/kg) and **1** (15 mg/kg) bid day 0-4 as compared with vehicle, in a A2780 xenograft mouse model.
40
41
42
43
44
45

46 Conclusion

47
48
49 The present study describes the successful discovery of novel NAMPT inhibitors with promising
50 biological activities as anti-proliferative agents in cancer cell lines in vitro and potent tumour reduction
51 efficacy in vivo in a xenograft mouse model. The structure based method used for the optimization of
52 these structures gave a rationale for the obtained activities and knowledge about the scope and limitation
53
54
55
56
57
58
59 in the design of new NAMPT inhibitors. The most active compounds in these new series compared
60

1 favorably, in respect to toxicology and in vivo activity, with compounds already in the clinic and
2 warrant further investigation as promising lead molecules for the inhibition of NAMPT.
3
4
5
6
7

8 **Experimentals**

9
10
11
12 Reaction conditions and yields were not optimized. ^1H and ^{13}C NMR spectra were recorded on a Bruker
13 Avance 300 spectrometer (300 MHz) or Varian 400 OXFORD NMR spectrometer (400 MHz).
14

15
16
17 Chemical shifts are reported in parts per million (δ) and referenced to hexamethyldisiloxane (HMDSO)
18 as an internal standard or using the signal according to deuterated solvent for ^1H spectra (CDCl_3 , 7.26;
19 CD_3OD , 3.31; $(\text{CD}_3)_2\text{SO}$, 2.50) and ^{13}C spectra (CDCl_3 , 77.23; CD_3OD , 49.00; $(\text{CD}_3)_2\text{SO}$, 39.52). The
20 value of a multiplet, either defined (doublet (d), triplet (t), double doublet (dd), double triplet (dt), quartet
21 (q)) or not (m) at the approximate mid-point is given unless a range is quoted. (bs) indicates a broad
22 singlet. MS was performed using an LC-MS using a Bruker Esquire 3000+ ESI Ion-trap with an Agilent
23 1200 HPLC-system or on an Acquity UPLC system (Waters) connected to the Micromass Q-TOF micro
24 hybrid quadrupole time of flight mass spectrometer operating in the electrospray ionization (ESI)
25 positive ion mode and using reverse-phase Acquity UPLC BEH C18 column (1.7 μm , 2.1 \times 50 mm) on a
26 gradient of 5-98% acetonitrile-water 0.1% formic acid. All tested compounds were of sufficient purity
27 (>95%) as determined by HPLC, using an Agilent 1200 HPLC-system. HRMS was carried out on a
28 Micromass *Q-Tof micro* mass spectrometer. Elemental analyses were performed on Carlo Erba CHNS-
29 O EA-1108 apparatus. Melting points were measured on a ‘‘Boetius’’ or Gallenkamp melting point
30 apparatus and are uncorrected. Silica gel, 0.035 e 0.070 mm, (Acros) was employed for column
31 chromatography.
32
33
34
35
36
37
38
39
40
41
42
43
44
45
46
47
48
49
50
51
52
53
54
55

56 **Preparation of key compounds 15 and 17.**

57
58
59
60

1 For a full description of the preparation and spectroscopic data of compounds reported in this paper
2
3 please view **Supporting Information**.
4
5

6 **6-(2-Cyano-3-(pyridin-4-yl)guanidino)-N-cyclohexyl-N-(2-morpholinoethoxy)hexane-1-**
7
8 **sulfonamide (15)**
9

10 **2-(2-Morpholinoethoxy)isoindoline-1,3-dione (XIVc)**

11
12 Synthesis of compound **XIVc** by modified version of published procedures⁴⁶⁻⁴⁸ was performed as
13 follows: To a mixture of 2-hydroxyisoindoline-1,3-dione (33.92 g, 208 mmol) and 4-(2-
14 chloroethyl)morpholine hydrochloride (50.24 g, 270 mmol) in 1-methyl-2-pyrrolidinone (160 ml)
15 slowly was added DBU (80 ml, 535 mmol) and the resulting mixture was stirred at 45°C for 6 h. The
16 mixture was poured into water (500 ml), extracted with ethyl acetate (3 × 250 ml), the combined extract
17 was washed with brine (200 ml), and dried (Na₂SO₄). The solvent was evaporated and the residue was
18 dried in vacuo to give compound **XIVc** (39.0 g, 68%) as an oil which solidified on standing. ¹H NMR
19 (200 MHz, CDCl₃) δ 2.50 (m, 4H), 2.79 (t, *J* = 5.5 Hz, 2H), 3.59 (m, 4H), 4.37 (t, *J* = 5.5 Hz, 2H), 7.70-
20 7.89 (m, 4H).
21
22
23
24
25
26
27
28
29
30
31
32
33

34 ***O*-(2-Morpholinoethyl)hydroxylamine (VIIIe)**

35
36 To a solution of 2-(2-morpholinoethoxy)isoindoline-1,3-dione (**XIVc**) (39.0 g, 141 mmol) in a mixture
37 of methanol (200 ml) and dichloromethane (100 ml) was added hydrazine hydrate (20 ml, 411 mmol)
38 and the obtained mixture was stirred at room temperature overnight. The resulting precipitate was
39 filtered off and the filtrate was concentrated in vacuo. The residue (22.9 g) was mixed with water (200
40 ml), to this mixture was added conc. HCl (30 ml), and the solid material was filtered off. The filtrate
41 was washed with EtOAc (200 ml) and the pH of the medium was raised to 10 by adding 5N aqueous
42 NaOH. The mixture was extracted with chloroform (3 × 300 ml), the extract was washed with brine
43 (100 ml), and dried (Na₂SO₄). The solvent was evaporated and the residue was dried in vacuo to give *O*-
44 (2-morpholinoethyl)hydroxylamine (**VIIIe**) (20.7 g, quantitative yield). ¹H NMR (200 MHz, CDCl₃) δ:
45 2.44-2.55 (m, 4H); 2.59 (t, *J* = 5.4 Hz, 2H); 3.69-3.77 (m, 4H); 3.81 (t, *J* = 5.4 Hz, 2H); 5.50 (b s, 2H).
46
47
48
49
50
51
52
53
54
55
56
57
58
59
60

Cyclohexanone *O*-(2-morpholin-4-ylethyl)oxime (XIXd)

To a stirred solution of cyclohexanone oxime (**XVIIc**) (22.64 g, 0.2 mol) in dimethylformamide (200 ml) at ice-bath temperature 60% sodium hydride in mineral oil (16.0 g, 0.4 mol) was added portion-wise and the resulting mixture was stirred at this temperature for 1 h. To the reaction mixture was added a suspension of 4-(2-chloroethyl)morpholine (37.22 g, 0.2 mol) in dimethylformamide (100 ml). The ice-bath was removed, the reaction mixture was stirred at room temperature for 16 h and at 60 °C for 3 h. The mixture was allowed to cool to room temperature, and then filtered and the filtrate was evaporated. The residue was mixed with a saturated ammonium chloride solution in water (300 ml) and extracted with diethyl ether (3 × 200 ml). The combined organic extracts were washed successively with 0.5 N sodium hydroxide (200 ml), brine (200 ml), and dried (Na₂SO₄). The solvent was evaporated and the residue (36.47 g) was chromatographed on silica gel (250 g) with chloroform-methanol (40 : 1) as eluent to give compound **XIXd** (35.1 g, 77.5%) as a yellow oil. ¹H NMR (400 MHz, CDCl₃) δ 1.54-1.71 (m, 6H), 2.18 (m, 2H), 2.43 (m, 2H), 2.52 (m, 4H), 2.66 (t, 2H, *J* = 5.8 Hz), 3.71 (m, 4H), 4.15 (t, 2H, *J* = 5.8 Hz).

4-{2-[(Cyclohexylamino)oxy]ethyl}morpholine (VIIIc)

To a solution of cyclohexanone *O*-(2-morpholin-4-ylethyl)oxime (**XIXd**) (13.9 g, 61.4 mmol) in methanol (100 ml) at ice-bath temperature were added sodium cyanoborohydride (7.72 g, 122.8 mmol) and trace of Methyl Orange. To the obtained slightly yellow solution slowly 2N HCl solution in methanol was added until the color of the reaction mixture changed from yellow to pink (in about 15 min.). The reaction mixture was stirred at room temperature for 5 h and the solvent was evaporated. To the residue was added water (30 ml) and the pH of the obtained solution was raised to pH>9 with 6N KOH, saturated with sodium chloride. The obtained mixture was extracted with chloroform (3 × 150 ml), the combined organic extract was washed with brine (100 ml), and dried (Na₂SO₄). The solvent was removed and the residue was dried in vacuo to afford title compound **VIIIc** (13.0 g, 92%) as a yellow oil. ¹H NMR (400 MHz, CDCl₃) δ 1.00-1.33 (m, 5H), 1.62 (m, 1H), 1.73 (m, 2H), 1.84 (m, 2H),

1 2.48 (m, 4H), 2.56 (t, 2H, $J = 5.7$ Hz), 2.84 (tt, 1H, $J = 3.7, 10.5$ Hz), 3.71 (m, 4H), 3.81 (t, 2H, $J = 5.7$
2 Hz), 5.43 (br s, 1H). LCMS (ESI) m/z : 299 $[M+H]^+$.

3 4 5 **Sodium 6-(1,3-dioxo-1,3-dihydro-2*H*-isoindol-2-yl)-1-hexanesulfonate (XXIVb)**

6 7 To a hot solution of 2-(6-bromohexyl)-1*H*-isoindole-1,3(2*H*)-dione (XXIIIb)⁴⁹ (12.67 g, 40.8 mmol) in
8 ethanol (82 ml) was added a solution of sodium sulfite (10.3 g, 81.7 mmol) in water (80 ml) and the
9 resulting mixture was refluxed overnight. The hot mixture was filtrated, crystallized from ethanol, and
10 dried in vacuo over P₂O₅ to give compound XXIVb (8.43 g, 62%). ¹H NMR (200 MHz, (CD₃)₂SO) δ
11 1.16-1.41 (m, 4H), 1.41-1.68 (m, 4H), 2.37 (m, 2H), 3.56 (t, 2H, $J = 7.0$ Hz), 7.77-7.92 (m, 4H). LCMS
12 (ESI): m/z 312 $[M_{\text{sulfonic acid}} + H]^+$.

13 14 15 **6-(1,3-Dioxo-1,3-dihydro-isoindol-2-yl)-hexanesulfonyl chloride (XXVb)**

16 17 A mixture of sodium 6-(1,3-dioxo-1,3-dihydro-2*H*-isoindol-2-yl)-1-hexanesulfonate (XXIVb) (13.99 g,
18 42.0 mmol) and phosphorus pentachloride (28.0 g, 134.5 mmol) was carefully ground in a mortar
19 (Caution – a good hood has to be used!). An evaluation of some amount of gas was observed and
20 gradually (in 2-3 min.) the solid mixture turned into an oily liquid. The obtained liquid was mixed with
21 toluene (280 ml), the precipitated solid material was filtered off, washed with toluene, and the filtrates
22 were combined. The solvent was evaporated and the residue was azeotropically dried several times with
23 toluene. The obtained white solid was dissolved in ethyl acetate (300 ml), washed successively with
24 water (100 ml), saturated sodium bicarbonate (2 \times 100 ml), brine (2 \times 100 ml), and dried (Na₂SO₄). The
25 solvent was evaporated and the residue was dried in vacuo over P₂O₅ to afford compound XXVb (10.4
26 g, 75%) as white crystals: mp 73-75°C. ¹H NMR (400 MHz, CDCl₃) δ 1.41 (qui, 2H, $J = 7.6$ Hz), 1.55
27 (qui, 2H, $J = 7.6$ Hz), 1.72 (qui, 2H, $J = 7.4$ Hz), 2.04 (m, 2H); 3.65 (m, 2H); 3.69 (t, 2H, $J = 7.1$ Hz);
28 7.67-7.75 (m, 2H); 7.80-7.87 (m, 2H). Anal. Calcd. for C₁₄H₁₆ClNO₄S: C, 50.99; H, 4.89; N, 4.25; S,
29 9.72. Found: C, 51.03; H, 5.01; N, 4.17; S, 9.68.

30 31 32 ***N*-Cyclohexyl-6-(1,3-dioxo-1,3-dihydro-2*H*-isoindol-2-yl)-*N*-(2-morpholinoethoxy)-1- 33 hexanesulfonamide (XXVIe)**

1 A solution of *N*-cyclohexyl-*O*-(2-morpholin-4-yl-ethyl)-hydroxylamine (**VIIIc**) (12.56 g, 55 mmol) and
2 triethylamine (14.0 ml, 100 mmol) in dry dichloromethane (100 ml) under argon atmosphere was cooled
3 to -20°C. To the stirred solution slowly during 1 h was added a solution of 6-(1,3-dioxo-1,3-dihydro-
4 2*H*-isoindol-2-yl)hexane-1-sulfonyl chloride (**XXVb**) (16.49 g, 50 mmol) in dichloromethane (50 ml),
5 and the resulting mixture was stirred at -20 °C for 20 h. The reaction mixture was concentrated to a
6 small volume, filtered, and the precipitated solid material was washed with dichloromethane. The
7 filtrate was evaporated, the residue (32.25 g) was dissolved in a small volume of chloroform and
8 chromatographed on silica gel (450 g) with hexane-isopropanol (gradient from 7:3 to 6:4) as eluent. The
9 eluate, containing pure product by TLC, was separated, and the impure material was re-
10 chromatographed using the same eluent. The eluates with TLC pure material were combined, the
11 solvent was evaporated, and the residue was dried in vacuo to afford compound **XXVIe** (16.4 g, 62.8%)
12 as a crystalline solid. ¹H NMR (400 MHz, CDCl₃) δ 1.10 (tq, 1H, *J* = 3.5, 12.9 Hz), 1.20-1.44 (m, 4H),
13 1.44-1.76 (m, 7H), 1.76-1.95 (m, 6H), 2.49 (m, 4H), 2.58 (t, 2H, *J* = 5.6 Hz), 3.08 (b s, 2H); 3.58 (tt,
14 1H, *J* = 3.6, 11.7 Hz), 3.68 (t, 2H, *J* = 7.0 Hz), 3.69 (m, 4H), 4.12 (b s, 2H), 7.71 (m, 2H), 7.83 (m, 2H).
15
16
17
18
19
20
21
22
23
24
25
26
27
28
29
30
31
32

33 **6-Amino-*N*-cyclohexyl-*N*-(2-morpholinoethoxy)-1-hexanesulfonamide (Ve)**

34
35
36 *N*-Cyclohexyl-6-(1,3-dioxo-1,3-dihydro-2*H*-isoindol-2-yl)-*N*-(2-morpholinoethoxy)-1-
37 hexanesulfonamide (**XXVIe**) (17.608 g, 33.75 mmol) was dissolved in a mixture of chloroform (150
38 ml) and absolute ethanol (150 ml), and hydrazine hydrate (4.2 ml, 86.54 mmol) was added. The
39 obtained mixture was refluxed for 5 h, and then stirred at room temperature overnight. The mixture was
40 filtered, the precipitate was washed with dichloromethane, and the combined filtrates were evaporated.
41 The residue was dissolved in dichloromethane (50 ml) and the mixture was kept in a refrigerator (*ca* 5
42 °C) for 1 h, and then filtered again. The filtrate was evaporated and the residue (14.392 g) was
43 chromatographed on silica gel (200 g) with methanol-30% ammonium hydroxide aqueous solution
44 (gradient from 25:1 to 20:1) to give 8.38 g of an oil. The oil was dissolved in dichloromethane (100 ml),
45 washed successively with water (2 × 20 ml), brine (20 ml), and dried (Na₂SO₄). The solvent was
46 evaporated and the residue was dried in vacuo at 50 °C to give compound **Ve** (7.67 g, 63.8%) as a
47
48
49
50
51
52
53
54
55
56
57
58
59
60

1 yellow oil. ^1H NMR (400 MHz, CDCl_3) δ 1.10 (tq, 1H, $J = 3.4, 12.9$ Hz), 1.20-1.52 (m, 8H), 1.52-1.69
2 (m, 5H), 1.75-1.98 (m, 6H), 2.49 (m, 4H), 2.59 (t, 2H, $J = 5.6$ Hz), 2.70 (t, 2H, $J = 6.8$ Hz), 3.09 (b s,
3 2H); 3.59 (tt, 1H, $J = 3.6, 11.7$ Hz), 3.69 (m, 4H), 4.12 (b s, 2H). LCMS (ESI) m/z : 392 $[\text{M}+\text{H}]^+$. Anal.
4
5 Calcd for $\text{C}_{18}\text{H}_{37}\text{N}_3\text{O}_4\text{S} \cdot 0.15 \text{H}_2\text{O}$: C, 54.83; H, 9.54; N, 10.66; S, 8.13. Found: C, 54.86; H, 9.66; N,
6
7 10.63; S, 8.14.
8
9

10
11 **6-(2-Cyano-3-(pyridin-4-yl)guanidino)-*N*-cyclohexyl-*N*-(2-morpholinoethoxy)hexane-1-**
12
13 **sulfonamide (15)**
14

15
16 A mixture of 6-amino-*N*-cyclohexyl-*N*-(2-morpholinoethoxy)-1-hexanesulfonamide (**Ve**) (2.49 g, 6.4
17 mmol), 4-[(cyanoimino)(methylsulfanyl)methyl]aminopyridine (**IIIa**) (1.22 g, 6.3 mmol), triethylamine
18 (3 ml, 21.6 mmol), and 4-dimethylaminopyridine (0.1 g, 0.8 mmol) in dry pyridine (4 ml) was stirred at
19 75-80 °C for 5 h. The solvent was evaporated to dryness and the residue was chromatographed on silica
20 gel (150 g) with acetonitrile-water (10:1) as eluent to give compound **15** (1.8 g, 53%) as a foam together
21 with a less pure material (1.0 g, 29%) which can be purified repeatedly by column chromatography to
22 increase the yield of the process. ^1H NMR (200 MHz, $(\text{CD}_3)_2\text{SO}$) δ 0.79-1.66 (m, 13H); 1.66-1.96 (m,
23 5H); 2.38-2.47 (m, 4H); 2.47-2.60 (m, 2H, overlapped with DMSO); 3.12-3.33 (m, 4H); 3.39-3.54 (m,
24 1H); 3.52-3.63 (m, 4H); 4.02 (t, $J = 5.6$ Hz, 2H); 7.21 (d, $J = 5.3$ Hz, 2H); 7.87 (t, $J = 5.5$ Hz, 1H); 8.38
25 (d, $J = 5.6$ Hz, 2H); 9.41 (b s, 1H). HRMS m/z calcd for $\text{C}_{25}\text{H}_{42}\text{N}_7\text{O}_4\text{S}$ $[\text{M}+\text{H}]^+$, 536.3019; found,
26 536.2976.
27
28
29
30
31
32
33
34
35
36
37
38
39
40
41
42

43 **6-(2-Cyano-3-(pyridin-4-yl)guanidino)-*N*-(cyclohexylmethoxy)-*N*-(2-fluoroethyl)hexane-1-**
44 **sulfonamide (17)**
45

46
47 ***N*-(Cyclohexylmethoxy)-6-(1,3-dioxo-1,3-dihydro-2*H*-isoindol-2-yl)-1-hexanesulfonamide**
48
49 **(XXVIIc)**
50

51
52 To a solution of *O*-(cyclohexylmethyl)hydroxylamine (**VIIIId**) (1.1 g, 8.51 mmol) and triethylamine (2.3
53 ml, 16.55 mmol) in dry dichloromethane (40 ml) at ice-bath temperature slowly for 2 h was added 6-
54 (1,3-dioxo-1,3-dihydro-2*H*-isoindol-2-yl)hexane-1-sulfonyl chloride (**XXVb**) (3.08 g, 9.34 mmol)
55
56
57
58
59
60 portion-wise. The reaction mixture was allowed gradually to warm up to room temperature (for 1 h) and

1 evaporated. The residue was dissolved in ethyl acetate (100 ml), washed successively with water (2 × 15
2 ml), brine (30 ml), and dried (Na₂SO₄). The solvent was evaporated and the residue was dried in vacuo
3 over P₂O₅ to afford compound **XXVIIc** (3.2 g, 89%) as crystalline solid. ¹H NMR (400 MHz, CDCl₃) δ
4 0.86-1.00 (m, 2H), 1.08-1.30 (m, 3H), 1.33-1.44 (m, 2H), 1.46-1.57 (m, 3H), 1.61-1.77 (m, 7H), 1.75-
5 1.85 (m, 2H), 3.18 (m, 2H), 3.68 (t, 2H, *J* = 7.2 Hz), 3.80 (d, 2H, *J* = 6.2 Hz), 6.99 (s, 1H), 7.71 (m,
6 2H), 7.84 (m, 2H).

14 ***N*-(Cyclohexylmethoxy)-6-(1,3-dioxo-1,3-dihydro-2*H*-isoindol-2-yl)-*N*-(2-fluoroethyl)-1-**
15 **hexanesulfonamide (XXVIIi)**

16 To a solution of *N*-(cyclohexylmethoxy)-6-(1,3-dioxo-1,3-dihydro-2*H*-isoindol-2-yl)-1-
17 hexanesulfonamide (**XXVIIc**) (2.11 g, 5.0 mmol), 2-fluoroethanol (0.4 g, 6.2 mmol), and
18 triphenylphosphine (2.16 g, 8.2 mmol) in dichloromethane (40 ml) at ice bath temperature slowly in 10
19 min. was added a solution of diethyl azodicarboxylate (1.43 g, 8.2 mmol) in dichloromethane (1.5 ml)
20 and the resulting mixture was stirred at this temperature for 20 min. The ice bath was removed, and then
21 the reaction mixture was stirred at room temperature for 3 h, and evaporated. The residue was mixed
22 with petroleum ether-ethyl acetate (4:1, 25 ml), the obtained suspension was stirred for 30 min. at ice
23 bath temperature and filtered. The filtrate was evaporated and the residue was chromatographed on
24 silica gel with toluene-ethyl acetate (9:1) as eluent to afford compound **XXVIIi** (1.57 g, 67%) as white
25 crystals. ¹H NMR (400 MHz, CDCl₃) δ 0.90-1.06 (m, 2H), 1.09-1.33 (m, 4H), 1.33-1.45 (m, 2H), 1.45-
26 1.79 (m, 9H), 1.83-1.95 (m, 2H), 3.07 (m, 2H), 3.54 (td, 2H, *J* = 5.0, 23.8 Hz), 3.68 (t, 2H, *J* = 7.1 Hz),
27 3.86 (d, 2H, *J* = 6.4), 4.62 (td, 2H, *J* = 5.0, 47.1 Hz), 7.71 (m, 2H), 7.83 (m, 2H).

28 **6-Amino-*N*-(cyclohexylmethoxy)-*N*-(2-fluoroethyl)-1-hexanesulfonamide (Vi)**

29 *N*-(Cyclohexylmethoxy)-6-(1,3-dioxo-1,3-dihydro-2*H*-isoindol-2-yl)-*N*-(2-fluoroethyl)-1-
30 hexanesulfonamide (**XXVIIi**) (1.53 g, 3.26 mmol) was dissolved in a mixture of ethanol (20 ml) and
31 chloroform (10 ml), and hydrazine hydrate (0.5 ml, 103 mmol) was added. The reaction mixture was
32 stirred at 60 °C for 2 h, left overnight at room temperature, and cooled in the refrigerator (5 °C). The
33 precipitated solid was filtered off and the filtrate was evaporated. The residue was chromatographed on
34
35
36
37
38
39
40
41
42
43
44
45
46
47
48
49
50
51
52
53
54
55
56
57
58
59
60

1 silica gel with chloroform-methanol-30% ammonium hydroxide aqueous solution (5:1:0.15) as eluent to
2 give compound **Vi** (0.93 g, 84%) as white crystals. ¹H NMR (400 MHz, CDCl₃) δ 0.90-1.04 (m, 2H),
3 1.09-1.30 (m, 3H), 1.33-1.54 (m, 6H), 1.54-1.78 (m, 6H), 1.82-2.02 (m, 4H), 2.72 (t, 2H, *J* = 6.9 Hz),
4 3.08 (m, 2H), 3.54 (td, 2H, *J* = 5.0, 23.6 Hz), 3.87 (d, 2H, *J* = 6.5), 4.62 (td, 2H, *J* = 5.0, 47.0 Hz).
5
6
7
8

9
10 **6-(2-Cyano-3-(pyridin-4-yl)guanidino)-*N*-(cyclohexylmethoxy)-*N*-(2-fluoroethyl)hexane-1-**
11 **sulfonamide (17)**

12
13 A mixture of 6-amino-*N*-(cyclohexylmethoxy)-*N*-(2-fluoroethyl)-1-hexanesulfonamide (**Vi**) (1.95 g,
14 5.76 mmol), 4-[(cyanoimino)(methylsulfanyl)methyl]aminopyridine (**IIIa**) (1.1 g, 5.76 mmol),
15 triethylamine (0.93 ml, 6.68 mmol), and 4-dimethylaminopyridine (0.15 g, 1.22 mmol) in dry pyridine
16 (20 ml) was stirred at 85 °C for 20 h. The solvent was evaporated to dryness; the residue was
17 azeotropically dried with toluene (2 × 5 ml), and then vigorously stirred with ether (30 ml) until the
18 precipitation occurred (*ca* 2h). The obtained suspension was filtered and the solid material (2.7 g) was
19 chromatographed on silica gel with chloroform-methanol-30% ammonium hydroxide aqueous solution
20 (6:1:0.015) as eluent to give compound **17** (2.48 g, 89%) as white crystals: mp 100-102 °C. ¹H NMR
21 (400 MHz, CDCl₃) δ 0.90-1.04 (m, 2H), 1.11-1.29 (m, 3H), 1.41 (qui, 2H, *J* = 7.3 Hz), 1.48-1.75 (m,
22 10H), 1.91 (qui, 2H, *J* = 7.6 Hz), 3.09 (t, 2H, *J* = 7.5 Hz), 3.36 (q, 2H, *J* = 6.6 Hz), 3.52 (dt, 2H, *J* = 4.9,
23 24.0 Hz), 3.86 (d, 2H, *J* = 6.5 Hz), 4.61 (dt, 2H, *J* = 4.9, 47.0 Hz), 5.51 (b s, 1H), 7.20 (d, 2H, *J* = 4.9
24 Hz), 7.68 (b s, 1H), 8.55 (d, 2H, *J* = 4.9 Hz). Anal. Calcd for C₂₂H₃₅FN₆O₃S: C, 54.75; H, 7.31; N,
25 17.41. Found: C, 54.85; H, 7.42; N, 17.50. HRMS *m/z* calcd for C₂₂H₃₆FN₆O₃S [M+H]⁺, 483.2554;
26 found, 483.2526.
27
28
29
30
31
32
33
34
35
36
37
38
39
40
41
42
43
44
45
46
47
48
49

50 **Cell culture**

51
52
53 Human breast carcinoma, MCF-7 and ovarian carcinoma A2780 were grown according to American
54 Type Culture Collection guidelines. Cell culture media were from Invitrogen unless otherwise stated.
55
56 MCF-7 was maintained in DMEM and A2780 in RPMI 1640 with GlutaMax. Media was supplemented
57
58
59
60

1 with 10%(v/v) FCS (Perbio, Thermo Fischer Scientific) and penicillin (100 U/mL), streptomycin (0.1
2 mg/mL) and cells incubated at 37 °C in an atmosphere containing 5% CO₂.
3
4
5
6

7 **WST-1 proliferation assay**

8
9 Cells were seeded in 96-well plates (3×10^3 cells/well) in culture medium (100 μ L). The following day
10 compounds were serially diluted in culture medium and 100 μ L of each dilution were added per well in
11 triplicate to the cell culture plates. Plates were incubated (72 h, 37°C, 5% CO₂ atmosphere) and the
12 number of viable cells assessed using cell proliferation reagent WST-1 (Roche, Mannheim, Germany).
13 Reagent (10 μ L) was added to each well and after a 1 h incubation period, absorbance was measured at
14 450 nm subtracting absorbance at 690 nm as a reference. Data were analysed using GraphPad Prism
15 (GraphPad Software, CA, USA) and CalcuSyn (Biosoft, Cambridge, UK) as appropriate.
16
17
18
19
20
21
22
23
24
25
26

27 **Clonogenic assays**

28
29 HCT-116/APO866 resistant cell line was obtained as described previously.⁴³
30
31

32 In vitro colony forming assays were performed essentially as previously published.⁵⁰ Briefly, HCT116
33 cells were cultured with compounds for the indicated times and seeded onto 35 mm dishes in agar (3%
34 (w/v)) containing a sheep erythrocyte feeder layer. Agar plates were cultured for 14–21 days at 37 °C
35 and colonies counted using a digital colony counter and Sorcerer image analysis software (Perceptive
36 Instruments Ltd, SuVolk, UK). Data were analyzed using GraphPad Prism (GraphPad Software, CA,
37 USA) and CalcuSyn (Biosoft, Cambridge, UK) as appropriate.
38
39
40
41
42
43
44
45
46
47

48 **NAMPT enzyme assay**

49
50 NAMPT enzyme activity was measured as described previously with minor modifications.^{51,52} In this
51 procedure the NAMPT catalysed formation of ¹⁴C-nicotinamide mononucleotide (NMN) was
52 determined, using ¹⁴C-nicotinamide and 5-phosphoribosyl-1-pyrophosphate (PRPP) as substrates.
53
54
55
56
57
58
59
60

1 For preparation of lysates, confluent HepG2 cells were washed twice with PBS (4°C, Ca²⁺, Mg²⁺ free),
2
3 once with NaHPO₄-buffer, (0.01 N, pH 7.4) and scraped in NaHPO₄-buffer. After centrifugation (10
4
5 min, 500×g, 4°C) pelleted cells were resuspended by pipetting in NaHPO₄-buffer to a concentration of
6
7 approx. 10⁷ cells/100 μl for HepG2 and aliquoted (200 μl aliquots in 2 ml tubes). Cells were then
8
9 broken up by sonography on ice (Bandelin Sonopuls, 3×10s, approx. 30% power). Cell debris was
10
11 removed by centrifugation (23,000×g, 90 min, 0°C). Protamine sulphate solution (1% in NaHPO₄
12
13 buffer) was added to the supernatant (70 μl/ml supernatant) to precipitate DNA by incubation on ice for
14
15 15 min. After centrifugation (23,000×g, 30 min, 0°C), aliquots of the supernatant were stored at -80°C.
16
17
18
19

20 Various concentrations of inhibitor or adequate concentrations of DMSO as solvent control and cell
21
22 lysates (10 μl) were added to a total of 50 μl reaction mixture (50 mmol/l TrisHCl pH 7.4; 2 mmol/l
23
24 ATP; 5 mmol/l MgCl₂; 0.5 mmol/l PRPP; 6.2 μmol/l ¹⁴C-nicotinamide; American Radiolabelled
25
26 Chemicals, St. Louis; MO, USA) and incubated (37°C, 1h). The reaction was terminated by transfer into
27
28 tubes containing acetone (2 ml). The whole mixture was then pipetted onto acetone-pre-soaked glass
29
30 microfiber filters (GF/A Ø 24 mm; Whatman, Maidstone, UK). After rinsing with acetone (2×1 ml),
31
32 filters were dried, transferred into vials with scintillation cocktail (6 ml, Betaplate Scint, PerkinElmer,
33
34 Waltham, MA, USA) and radioactivity of ¹⁴C-NMN was quantified in a liquid scintillation counter
35
36 (Wallac 1409 DSA, Perkin Elmer). After subtraction of blank values, NAMPT activity was normalized
37
38 to total protein as measured by BCA assay (Pierce).
39
40
41
42
43
44
45

46 **Xenograft studies**

47
48 The anti-tumour effect in vivo was tested in an A2780 (ovarian cancer) subcutaneous (s.c.) xenograft
49
50 model in nude mice (female, NMRI/nude, Harlan or Taconic). Cancer cells were grown in RPMI + 10%
51
52 FBS, washed once with PBS and suspended in 100 μL of PBS + 100 μL matrigel (BD) and injected s.c.
53
54 Treatment started at tumour volumes around 100 mm³ (small tumours) or 500 mm³ (large tumour). The
55
56 compounds were formulated in DMSO 2%, 20% HP-β-CD and isotonic saline at 10 mL/kg i.p.
57
58
59
60

1 injection. Tumour diameters were measured during tumour growth and tumour volumes (T_v) estimated
2 according to the formula: $T_v = (\text{width}^2 \times \text{length})/2$. Mice were observed for tumour regression after 1
3 week or else sacrificed. The experiments were conducted at Topotarget A/S, Copenhagen and approved
4 by the Experimental Animal Inspectorate, Danish Ministry of Justice.
5
6
7
8

9 10 11 **Pharmacokinetic analysis**

12 Mouse plasma samples were prepared for analysis by protein precipitation on Sirocco plates (Waters,
13 Milford, Ma, USA). Waters Acquity UPLC system with Quattro Premier MS-MS system was used for
14 separation and detection. Acetonitrile containing 1 $\mu\text{g/ml}$ of internal standard was used in the ratio 3:1
15 (v/v) for precipitation. Separation was performed with an acetonitrile – 0.05% formic acid gradient on a
16 Acquity UPLC BEH C18, 2.1 \times 50 mm, 1.7 μm reversed phase column (Waters A/S) operated at 40°C.
17
18
19
20
21
22
23
24
25
26
27
28
29
30
31
32
33
34
35
36
37
38
39
40
41
42
43
44
45
46
47
48
49
50
51
52
53
54
55
56
57
58
59
60
Detection was performed using electrospray MRM in the positive mode. Pharmacokinetic parameters
were calculated using non compartmental analysis methods as included in WinNonlin ver 5.02
(Pharsight, CA, USA).

36 **Docking analysis**

37
38
39
40
41
42
43
44
45
46
47
48
49
50
51
52
53
54
55
56
57
58
59
60
The structure was downloaded from the protein data bank (PDB ID 2GVJ) and prepared for docking
using the built-in protein preparation wizard in Maestro v. 9.3. During this process bond orders were
assigned and hydrogens added to the crystal structure. Furthermore, the four seleno-methionines which
had been incorporated to allow for better X-ray diffraction were changed to cysteines (chain A: residues
368 and 372, chain B: residues 368 and 372). The docking was carried out using Glide v. 5.8 in extra
precision (XP) mode. The ligands were docked flexibly and nitrogen inversions and ring flips were
allowed. The van der Waals radii of the non-polar ligand atoms (partial charge < 0.15) were scaled by a
factor of 0.8 to accommodate slightly inaccurate initial dockings. A post-docking minimization was
carried out for the best 25 poses for each ligand and finally the 10 best poses were reported.

DFT analysis

This study was carried out using Jaguar v. 8.0.⁵³ DFT using the B3LYP functional⁵⁴⁻⁵⁶ with added d3 corrections^{57,58} to account for dispersion interactions. We used the 6-31G** basis set⁵⁹ throughout.

Supporting Information Available. Experimental procedures, analytical and spectral data for all intermediate and final compounds, computation chemistry docking scores and associated docking poses.

This material is available free of charge via the Internet at <http://pubs.acs.org>.

Corresponding Author

*Fredrik Björkling, Department of Drug Design and Pharmacology, Faculty of Health and Medical Sciences, University of Copenhagen, Universitetsparken 2, DK-2100 Copenhagen, Denmark, fb@sund.ku.dk, phone; +45 35 33 62 31, fax; +45 35 33 60 41

Present Address

M.K.C., Novo Nordisk A/S, 2880 Bagsværd, Denmark. A.T., H. Lundbeck A/S, 2500 Valby, Denmark. S.J.N., Nuevolotion A/S 2100 Copenhagen, Denmark. P.B.J., Medical Prognosis Institute, 2970 Hørsholm, Denmark.

Notes

Authors K.D.E. and J.T. are employees of Topotarget A/S. Authors M.K.C., U.H.O., A.T., S.J.N., M.S., P.B.J. and F.B. are previous employees of Topotarget A/S.

Acknowledgment

1 We thank Anja Barnikol-Oettler for expert technical assistance with the NAMPT enzymatic assay and
2 support from the German Research Council (DFG, KFO152-TP7) and the Leipzig LIFE (LIFE Child
3 Health and Child Obesity) program to W.K. P.F. was supported by a Sapare Aude grant from the Danish
4 Council for Independent Research no. 11-105487. We thank Nicolaj Høj and Søren Ryborg for organic
5 synthesis assistance.
6
7
8
9
10

11 Abbreviations

12
13
14 cADPR, cyclic ADP ribose ; NAADP, nicotinic acid adenine dinucleotide phosphate; AUC, area under
15 the curve; bid, twice daily; DMEM, Dulbecco's modified eagle medium; HRMS, high resolution mass
16 spectrometry; IC₅₀, concentration of a test compound that produces half maximal inhibition; LC-MS,
17 liquid chromatography - mass spectrometry; MTD, maximum tolerated dose; T_{max}, time of maximum
18 drug concentration; C_{max}, maximum drug concentration; Vz, volume of distribution; CL, drug clearance;
19 NMR, nuclear magnetic resonance; SAR, structure-activity relationship; SD, standard deviation
20
21
22
23
24
25
26
27
28
29
30
31

32 References

- 33
34
35 1. Khan, J.A.; Forouhar, F.; Tao, X.; Tong, L. Nicotinamide adenine dinucleotide metabolism as
36 an attractive target for drug discovery *Expert Opin. Ther. Tar.* **2007**, *11*(5), 695-705.
37
38 2. Diefenbach, J.; Burkle, A. Introduction to poly(ADP-ribose) metabolism. *Cell Mol. Life Sci.* **2005**,
39 *62*(7-8), 721–730.
40
41 3. Ziegler, M. New functions of a long-known molecule. Emerging roles of NAD in cellular signaling.
42 *Eur. J. Biochem.* **2000**, *267*(6), 1550–1564.
43
44 4. Saunders, L. R.; Verdin, E. Sirtuins: critical regulators at the crossroads between cancer and aging.
45 *Oncogene* **2007**, *26*(37), 5489–5504.
46
47 5. Genazzani, A. A.; Billington, R. A. NAADP: an atypical Ca²⁺ - release messenger? *Trends*
48 *Pharmacol. Sci.* **2002**, *23*, 165–167.
49
50
51
52
53
54
55
56
57
58
59
60

- 1
2
3
4
5
6
7
8
9
10
11
12
13
14
15
16
17
18
19
20
21
22
23
24
25
26
27
28
29
30
31
32
33
34
35
36
37
38
39
40
41
42
43
44
45
46
47
48
49
50
51
52
53
54
55
56
57
58
59
60
6. Malavasi, F.; Deaglio, S.; Funaro, A.; Ferrero, E.; Horenstein, A. L.; Ortolan, E.; Vaisitti, T.; Aydin, S. Evolution and function of the ADP ribosyl cyclase/CD38 gene family in physiology and pathology. *Physiol. Rev.* **2008**, *88*, 841–886.
7. Hageman, G. J.; Stierum, R. H. Niacin, poly(ADP-ribose) polymerase-1 and genomic stability. *Mutat. Res.* **2001**, *475*(1-2), 45–56.
8. Lengauer, C.; Kinzler, K. W.; Vogelstein, B. Genetic instabilities in human cancers. *Nature* **1998**, *396*(6712), 643–649.
9. Nomura, F.; Yaguchi, M.; Togawa, A.; Miyazaki, M.; Isobe, K.; Miyake, M.; Noda, M.; Nakai, T. Enhancement of poly-adenosine diphosphate-ribosylation in human hepatocellular carcinoma. *J. Gastroen. Hepatol.* **2000**, *15*(5), 529–535.
10. Hufton, S. E.; Moerkerk, P. T.; Brandwijk, R.; de Bruïne, A. P.; Arends, J-W.; Hoogenboom, H. R. A profile of differentially expressed genes in primary colorectal cancer using suppression subtractive hybridization. *FEBS Lett.* **1999**, *463*, 77-82.
11. van Beijnum, J. R.; Moerker, P.T.; Gerbers, A. J.; de Bruïne, A. P.; Arends, J-W.; Hoogenboom, H. R.; Hufton, S. E. Target validation for genomics using peptide-specific phage antibodies: a study of five gene products overexpressed in colorectal cancer. *Int. J. Cancer* **2002**, *101*, 118-127.
12. Foster, J. W.; Moat, A. G. Nicotinamide adenine dinucleotide biosynthesis and pyridine nucleotide cycle metabolism in microbial systems. *Microbiol. Rev.* **1980**, *44* (1), 83–105.
13. Magni, G.; Amici, A.; Emanuelli, M.; Orsomando, B.; Raffaelli, N.; Ruggieri, S. Enzymology of NAD⁺ homeostasis in man. *Cell. Mol. Life Sci.* **2004**, *61*(1), 19-34.
14. Preiss, J.; Handler, P. Enzymatic synthesis of nicotinamide mononucleotide. *J. Biol. Chem.* **1957**, *225*, 759-770.
15. Preiss, J.; Handler, P. Biosynthesis of diphosphopyridine nucleotide. I. Identification of intermediates. *J. Biol. Chem.* **1958**, *233*, 488-492.
16. Rongvaux, A.; Andris, F.; van Gool, F.; Leo, O. Reconstructing eukaryotic NAD metabolism. *Bioessays* **2003**, *25*, 683-690.

- 1 17. Gross, J.W.; Rajavel, M.; Grubmeyer, C. Kinetic mechanism of nicotinic acid
2 phosphoribosyltransferase: implications for energy coupling. *Biochem.* **1998**, *37*, 4189-4199.
- 3
4 18. Olesen, U.H., Hastrup, N., Sehested, M. Expression patterns of nicotinamide
5 phosphoribosyltransferase and nicotinic acid phosphoribosyltransferase in human malignant
6 lymphomas. *APMIS.* **2011**, *119*(4-5), 296-303.
- 7
8 19. Shackelford, R. E.; Bui, M. M.; Coppola, D.; Hakam, A. Over-expression of nicotinamide
9 phosphoribosyltransferase in ovarian cancers. *Int. J. Clin. Exp. Pathol.* **2010**, *3*(5), 522-527.
- 10
11 20. Wang, B.; Hasan, M. K.; Alvarado, E.; Huan, H.; Wu, H.; Chen, W. Y. NAMPT overexpression in
12 prostate cancer and its contribution to tumor cell survival and stress response. *Oncogene* **2011**,
13
14
15
16
17
18
19
20
21
22
23
24
25
26
27
28
29
30
31
32
33
34
35
36
37
38
39
40
41
42
43
44
45
46
47
48
49
50
51
52
53
54
55
56
57
58
59
60
21. Hasmann, M.; Schemainda, I. FK866, a highly specific noncompetitive inhibitor of nicotinamide
phosphoribosyltransferase, represents a novel mechanism for induction of tumor cell apoptosis.
Cancer Res. **2003**, *63*, 7436-7442.
22. Schou, C.; Ottosen, E. R.; Petersen, H. J.; Björkling, F.; Latini, S.; Hjarnaa, P.V.; Bramm, E.;
Binderup, L. Novel cyanoguanidines with potent oral antitumour activity. *Bioorg. Med. Chem.*
Lett., **1997**, *7*(24), 3095-3100.
23. Colombano, G.; Travelli, T.; Galli, U.; Caldarelli, A.; Chini, M. G.; Canonico, P. L.; Sorba, G.;
Bifulco, G.; Tron, G. C.; Genazzani A. A. A novel potent nicotinamide phosphoribosyltransferase
inhibitor synthesized via click chemistry. *J. Med. Chem.* **2010**, *53*, 616-623.
24. Fleischer, T. C.; Murphy, B. R.; Flick, J. S.; Terry-Lorenzo, R. T.; Gao, Z-H.; Davis, T.;
McKinnon, R.; Ostanin, K.; Willardsen, J. A.; Boniface, J. J. Chemical proteomics identifies Nampt
as the target of CB30865, an orphan cytotoxic compound. *Chem. Biol.* **2010**, *17*, 659-664.
25. Carlson, R. O.; Willardsen, J. A.; Lockman, J. W.; Bradford, C. L.; Patton, J. S.; Papac, D. I.;
Boniface, J. J.; Yager, K.; Baichwal, V. R. Pharmacokinetics, anti-tumor activity and therapeutic
index of Nampt inhibitor MPC-8640 in mice. *Mol. Cancer Ther.* **2011**, *10*(11 Suppl.), Abstract nr
B137.

- 1
2
3
4
5
6
7
8
9
10
11
12
13
14
15
16
17
18
19
20
21
22
23
24
25
26
27
28
29
30
31
32
33
34
35
36
37
38
39
40
41
42
43
44
45
46
47
48
49
50
51
52
53
54
55
56
57
58
59
60
26. Cea, M.; Zoppoli, G.; Bruzzone, S.; Fruscione, F.; Moran, E.; Garuti, A.; Rocco, I.; Cirmena, G.; Casciaro, S.; Olcese, F.; Pierri, I.; Cagnetta, A.; Ferrando, F.; Ghio, R.; Gobbi, M.; Ballestrero, A.; Patrone, F.; Nencioni, A. APO866 activity in hematologic malignancies: a preclinical in vitro study. *Blood* **2009**, *113*, 6035-6037.
 27. Nahimana, A.; Attinger, A.; Aubry, D.; Greaney, P.; Ireson, C.; Thougard, A. V.; Tjørnelund, J.; Dawson, K. M.; Dupuis, M.; Duchosal, M. A. The NAD biosynthesis inhibitor APO866 has potent antitumor activity against hematologic malignancies. *Blood* **2009**, *113*, 3276-3286.
 28. Galli, U.; Travelli, C.; Massarotti, A.; Fakhfour, G.; Rahimian, R.; Tron, G. C.; Genazzani, A. A. Medicinal chemistry of nicotinamide phosphoribosyltransferase (NAMPT) Inhibitors. *J. Med. Chem.* **2013**, *56* (16), 6279–6296.
 29. Olesen, U. H.; Christensen, M. K.; Björkling, F.; Jäättelä, M.; Jensen, P. B.; Sehested, M.; Nielsen, S. J. Anticancer agent CHS-828 inhibits cellular synthesis of NAD. *Biochem. Biophys. Res. Commun.* **2008**, *367*(4), 799-804.
 30. Watson, M.; Roulston, A.; Belec, L.; Billot, X.; Marcellus, R.; Bédard, D.; Bernier, C.; Branchaud, S.; Chan, H.; Dairi, K.; Gilbert, K.; Goulet, D.; Gratton, M-O.; Isakau, H.; Jang, A.; Khadir, A.; Koch, E.; Lavoie, M.; Lawless, M.; Nguyen, M.; Paquette, D.; Turcotte, E.; Berger, A.; Mitchell, M.; Shore, G.C.; Beauparlant, P. The Small Molecule GMX1778 Is a Potent Inhibitor of NAD_Biosynthesis: rategy for Enhanced Therapy in Nicotinic Acid Phosphoribosyltransferase 1-Deficient Tumors; *Mol. Cell. Biol.* **2009**, 5872–5888.
 31. Khan, J.A.; Tao, X.; Tong, L. Molecular basis for the inhibition of human NMPRTase, a novel target for anticancer agents. *Nat. Struct. Mol. Biol.* **2006**, *13*, 582-588.
 32. Holen, K.; Saltz, L. B.; Hollywood, E.; Burk, K.; Hanauske, A. R.. The pharmacokinetics, toxicities, and biologic effects of FK866, a nicotinamide adenine dinucleotide biosynthesis inhibitor. *Invest. New Drug.* **2008**, *26*, 45-51.

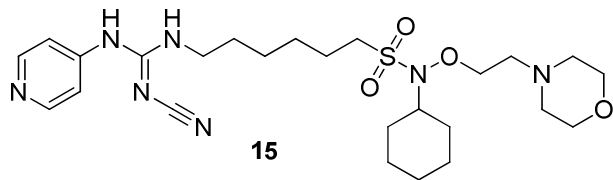
- 1
2
3
4
5
6
7
8
9
10
11
12
13
14
15
16
17
18
19
20
21
22
23
24
25
26
27
28
29
30
31
32
33
34
35
36
37
38
39
40
41
42
43
44
45
46
47
48
49
50
51
52
53
54
55
56
57
58
59
60
33. Hovstadius, P.; Larsson, R.; Jonsson, E.; Skov, T.; Kissmeyer, A. M.; Krasilniko, V. K.; Bergh, J.; Karlsson, M. O.; Lonnebo, A.; Ahlgren, J. A phase I study of CHS 828 in patients with solid tumour malignancy. *Clin. Cancer Res.* **2002**, *8*, 2843–2850.
34. Pishvaian, M.; Marshall, J.; Hwang, J.; Malik, S.; He, A.; Deeken, J.; Kelso, C.; Cotaria, I.; Berger, M. A. Phase I trial of GMX1777, an inhibitor of nicotinamide phosphoribosyl transferase (NAMPT), given as a 24-hour infusion. *J. Clin. Oncol.* ASCO Annual Meeting Proceedings (Post-Meeting Edition), **2008**, *26*, No 15S (May 20 Supplement).
35. Binderup, E.; Björkling, F.; Hjarnaa, P. V.; Latini, S.; Baltzer, B.; Carlsen, M.; Binderup L. EB1627: a soluble prodrug of the potent anticancer cyanoguanidine CHS828. *Bioorg. Med. Chem. Lett.* **2005**, *15*, 2491-2494.
36. Beauparlant, P.; Bédard, D.; Bernier, C.; Chan, H.; Gilbert, K.; Goulet, D.; Gratton, M-O.; Lavoie, M.; Roulston, A.; Turcotte, E.; Watson, M. Preclinical development of the nicotinamide phosphoribosyl transferase inhibitor prodrug GMX1777. *Anti-Cancer Drug.* **2009**, *20*, 346-354.
37. Skelton, L. A.; Ormerod, M. G.; Titley, J.; Kimbell, R.; Brunton, L. A.; Jackman, A. L. A novel class of lipophilic quinazoline-based folic acid analogues: cytotoxic agents with a folate-independent locus. *Br. J. Cancer* **1999**, *79*(11/12), 1692–1701.
38. Orwig, K. S.; Dix, T. A. Synthesis of C-alpha methylated carboxylic acids: isosteres of arginine and lysine for use as N-terminal capping residues in polypeptides. *Tetrahedron Lett.* **2005**, *46*(41), 7007-7009.
39. Butera, J. A.; Antane, M. M.; Antane, S. A.; Argentieri, T. M.; Freeden, C.; Graceffa, R. F.; Hirth, B. H.; Jenkins, D.; Lennox, J. R.; Matelan, E.; Norton, N. W.; Quagliato, D.; Sheldon, J. H.; Spinell, W.; Warga, D.; Wojdan, A.; Woods, M. Design and SAR of Novel Potassium Channel Openers Targeted for Urge Urinary Incontinence. 1. *N-Cyanoguanidine Bioisosteres Possessing in Vivo Bladder Selectivity.* *J. Med. Chem.* **2000**, *43*, 1187-1202.

- 1
2
3
4
5
6
7
8
9
10
11
12
13
14
15
16
17
18
19
20
21
22
23
24
25
26
27
28
29
30
31
32
33
34
35
36
37
38
39
40
41
42
43
44
45
46
47
48
49
50
51
52
53
54
55
56
57
58
59
60
40. Humljan, J.; Gobec, S. Synthesis of N-phthalimido b-aminoethanesulfonyl chlorides: the use of thionyl chloride for a simple and efficient synthesis of new peptidosulfonamide building blocks *Tetrahedron Lett.* **2005**, *43*, 4069-4072.
 41. Mun-Kyoung, K.; Lee, J. H.; Kim, H.; Park, S. J.; Kim, S. H.; Kang, G. B.; Lee, Y. S.; Kim, J. B.; Kim, K. K.; Suh, S. W.; Eom, S. H. Crystal structure of visfatin/pre-B cell colony-enhancing factor 1/ nicotinamide phosphorybosyltransferase, free and in complex with the anti-cancer agent FK-866. *J. Mol. Biol.* **2006**, *362*, 66-77.
 42. Kim, M. K.; Lee, J. H.; Kim, H.; Park, S. J.; Kim, S. H.; Kang, G. B.; Lee, Y. S.; Kim, J. B.; Kim, K.K.; Suh, S. W.; Eom, S. H. Crystal structure of visfatin/pre-B cell colony-enhancing factor 1/nicotinamide phosphoribosyltransferase, free and in complex with the anti-cancer agent FK-866. *J. Mol. Biol.* **2006**, *362*, 66-77.
 43. Olesen, U. H.; Petersen, J. G.; Garten, A.; Kiess, W.; Yoshino, J.; Imai, S.; Christensen, M. K.; Fristrup, P.; Thougard, A. V.; Björkling, F.; Jensen, P. B.; Nielsen, S. J.; Sehested, M. Target enzyme mutations are the molecular basis for resistance towards pharmacological inhibition of nicotinamide phosphoribosyltransferase. *BMC Cancer.* **2010**, *10*, 677.
 44. Murthi, K. K.; Köstler, R.; Smith, C.; Brandstetter, T.; Kluge, A. F. Derivatives of squaric acid with anti-proliferative activity. EU Pat. Appl. **2004** EP 1 674 457 A1
 45. Linderoth, L.; Fristrup, P.; Hansen, M.; Melander, F.; Madsen R.; Andresen, T. L.; Peters, G. H. Mechanistic Study of the sPLA₂-Mediated Hydrolysis of a Thio-ester Pro Anticancer Ether Lipid *J. Am. Chem. Soc.* **2009**, *131*, 12193-12200.
 46. Kornet, M.J. Potential antifibrillatory agents. N-(ω-aminoalkoxy) phthalimides. *J. Med. Chem.* **1966**, *9*, 269.
 47. Deraeve, C.; Bon, R. S.; Stigter, E. A.; Wetzel, S.; Waldmann, H.; Guo, Z.; Blankenfeldt, W.; Alexandrov, K.; Goody, R. S.; Wu, Y.W.; DiLucrezia, R.; Wolf, A.; Menninger, S.; Choidas, A. Psoromic Acid is a Selective and Covalent Rab-Prenylation Inhibitor Targeting Autoinhibited RabGGTase. *J. Am. Chem. Soc.* **2012**, *134*, 7384-7391.

- 1
2
3
4
5
6
7
8
9
10
11
12
13
14
15
16
17
18
19
20
21
22
23
24
25
26
27
28
29
30
31
32
33
34
35
36
37
38
39
40
41
42
43
44
45
46
47
48
49
50
51
52
53
54
55
56
57
58
59
60
48. BOEHRINGER INGELHEIM INTERNATIONAL GMBH, Patent: WO2009/112565 A1, **2009**.
49. Zhao, X.; Jiang, X. K.; Shi, M.; Yu, Y. H.; Xia, W.; Li, Z. T. Self-assembly of novel [3]- and [2]-rotaxanes with two different ring components: donor-acceptor and hydrogen bonding interactions and molecular-shuttling behavior. *J. Org. Chem.* **2001**, *66* (21), 7035-7043.
50. Natarajan, A.; Fan, Y.-H.; Chen, H.; Guo, Y.; Iyasere, J.; Harbinski, F.; Christ, W. J.; Aktas, H.; Halperin, J. A. 3,3-Diaryl-1,3-dihydroindol-2-ones as antiproliferatives mediated by translation initiation inhibition. *J. Med. Chem.* **2004**, *47*, 1882–1885.
51. Elliott, G. C.; Ajioka, J.; Okada, C. Y. A rapid procedure for assaying nicotinamide phosphoribosyl-transferase, *Anal. Biochem.* **1980**, *107*, 199-205.
52. Garten, A.; Petzold, S.; Barnikol-Oettler, A.; Körner, A.; Thasler, W.E.; Kratzsch, J.; Kiess, W.; Gebhardt, R. Nicotinamide phosphoribosyltransferase (NAMPT/PBEF/visfatin) is constitutively released from human hepatocytes. *Biochem. Biophys. Res. Co.* **2010**, *391*, 376-381.
53. Jaguar version 8.0 release 47, Schrodinger, LLC, New York, NY, 2013.
54. Becke, A. D. Density-functional thermochemistry. III. The role of exact exchange. *J. Chem. Phys.* **1993**, *98*, 5648–5652.
55. Becke, A. D. A new mixing of Hartree–Fock and local density-functional theories. *J. Chem. Phys.* **1993**, *98*, 1372–1377.
56. Lee, C.; Yang, W.; Parr, R. G. Development of the Colle-Salvetti correlation-energy formula into a functional of the electron density. *Phys. Rev. B* **1988**, *37*, 785–789.
57. Elstner, M.; Hobza, P.; Frauenheim, T.; Suhai, S.; Kaxiras, E. Hydrogen bonding and stacking interactions of nucleic acid base pairs: A density-functional-theory based treatment. *J. Chem. Phys.* **2001**, *114*, 5149–5155
58. Grimme, S. Accurate description of van der Waals complexes by density functional theory including empirical corrections. *J. Comput. Chem.* **2004**, *25*, 1463-1473.

- 1
2
3
4
5
6
7
8
9
10
11
12
13
14
15
16
17
18
19
20
21
22
23
24
25
26
27
28
29
30
31
32
33
34
35
36
37
38
39
40
41
42
43
44
45
46
47
48
49
50
51
52
53
54
55
56
57
58
59
60
59. Ditchfield, R.; Hehre, W. J.; Pople, J. A. Self-Consistent Molecular-Orbital Methods. IX. An Extended Gaussian-Type Basis for Molecular-Orbital Studies of Organic Molecules. *J. Chem. Phys.* **1971**, *54*, 724-728.

Table of Contents graphic



15

Biological Data: IC₅₀

0.025 nM in A2780

0.33 nM in MCF-7